Article

Fusarium proliferatum PSA-3 Produces Xylanase-Aggregate to Degrade Complex Arabinoxylan

Kanlaya Thattha , Lakha Salaipeth , Sangchai Akeprathumchai , Ken-Lin Chang , Takashi Watanabe , Paripok Phitsuwan *

Posted Date: 25 September 2025

doi: 10.20944/preprints202509.2067.v1

Keywords: *Fusarium proliferatum* PSA-3 1; xylanase aggregate, rice straw, arabinoxylan degradation

 doi:10.20944/preprints202509.2067.v1

Article

Fusarium proliferatum PSA-3 Produces Xylanase-Aggregate to Degrade Complex Arabinoxylan

Kanlaya Thattha [1,2], Lakha Salaipeth [1,3], Sangchai Akeprathumchai [1,4], Ken-Lin Chang [5], Takashi Watanabe [6] and Paripok Phitsuwan [1,2,*]

[1] *LigniTech*-Lignin Technology Research Group, School of Bioresources and Technology, King Mongkut's University of Technology Thonburi, Bangkuntien, Bangkok 10150, Thailand
[2] Division of Biochemical Technology, School of Bioresources and Technology, King Mongkut's University of Technology Thonburi, Bangkuntien, Bangkok 10150, Thailand
[3] Natural Resource Management and Sustainability Program, School of Bioresources and Technology, King Mongkut's University of Technology Thonburi, Bangkuntien, Bangkok 10150, Thailand
[4] Biotechnology Program, School of Bioresources and Technology, King Mongkut's University of Technology Thonburi, Bangkuntien, Bangkok 10150, Thailand
[5] Institute of Environmental Engineering, National Sun Yat-Sen University, Kaohsiung City, Taiwan
[6] Research Institute for Sustainable Humanosphere (RISH), Kyoto University, Uji, Kyoto 611-0011, Japan
* Correspondence: paripok.phi@kmutt.ac.th

Abstract

Xylanolytic enzymes of *Fusarium* species are closely associated with pathogenesis, where they soften plant cell walls to facilitate infection and nutrient uptake. This study investigated the xylanolytic system of *Fusarium proliferatum* PSA-3, a strain isolated from mango leaves showing dark spot symptoms. When cultivated on rice straw under solid-state fermentation, PSA-3 produced high xylanase activity against rye arabinoxylan (50.2 U) and beechwood xylan (56.8 U). Partial purification by ion-exchange and gel-filtration chromatography yielded a large xylanase aggregate (158 kDa), which appeared as a smear at the top of the gel under native conditions. Mild denaturation resolved the aggregate into at least four active proteins of ~20, 35, 48, and 63 kDa, indicating that multiple xylanases assemble into a functional aggregate. The aggregate retained activity across pH 4.0–8.0, with an optimum at pH 5.0 and 50 °C, and was resistant to Ni^{2+}, Fe^{2+}, Co^{2+}, and β-mercaptoethanol, but inhibited by SDS. Hydrolysis of xylo-oligosaccharides (DP 2–6), purified xylans, and plant-derived xylans confirmed predominantly endo-type action with debranching activity toward A2XX and A2,3XX. These findings reveal a natural xylanase aggregate in *F. proliferatum*, providing a potential mechanism for efficient degradation of arabinoxylan-rich cell walls and offering targets for antifungal strategies and biotechnological applications.

Keywords: *Fusarium proliferatum* PSA-3 1; xylanase aggregate; rice straw; arabinoxylan degradation

1. Introduction

Lignocellulose is a complex biopolymer composed of lignin (15–20%), cellulose (40–50%) and hemicellulose (25–30%) [1,2]. For land plants, xylan represents a major component of hemicellulose, and their structures vary depending on the plant species and plant tissues. In general, xylan is a heterogeneous polysaccharide with a backbone of β-(1,4)-linked D-xylosyl residues containing numerous side-groups connected to the main chain. α-Glucuronic acid (GlcA) and/or 4-O-methyl-α-glucuronic acid (MeGlcA) side groups are substituted on the xylan main chains to form glucuronoxylan, and this kind of xylans is typically found in dicots [3]. In cereal grains, xylan main chains, particularly in wheat and rye kernels, are frequently decorated with arabinofuranoses suited at α-(1,2) or α-(1,3), or both of which, on a xylose moiety, giving monosubstituted and disubstituted xylose residues [4]. This xylan is thus classed as arabinoxylan. In addition, the more complicated

 doi:10.20944/preprints202509.2067.v1

xylan is known as glucuronoarabinoxylan, which is found in grasses and gymnosperms. Arabinofuranoses, with a small amount of GlcA, often link to xylan backbones at α-(1,2) or α-(1,3) positions on the xylose residues, and the α-(1,2) and α-(1,3)-linked arabinofuranoses may be further substituted with xylose, coumaric acid, or ferulic acid [3,5]. This additional substitution is important for organizing cell wall architecture and biological function. It has been shown that grass glucuronoarabinoxylans crosslinked with lignin through ferulate linkages to form ferulate-polysaccharide-lignin complex [6]. This complex is to provide strength to plant cell walls and resistance to diseases and pathogenesis [5].

Because of the structural heterogeneity and complexity, degradation of xylan requires several enzymes with various modes of action. It has been assumed that different types of depolymerizing β-(1,4)-endoxylanases that act upon internal xylan main chains work in concert with β-(1,4)-xylosidases and debranching enzymes such as acetylxylanesterases, feruloylesterases, α-glucuronidase, and α-L-arabinofuranosidase in breakdown of complex highly branched xylans [2]. In nature, several microorganisms produce repertoire of xylanolytic enzymes, which are cell-associated or secreted to environment, to degrade xylan [7,8]. Filamentous fungi have been reported to produce a higher level of extracellular xylanolytic enzymes than bacteria and yeast [9]. Furthermore, β-(1,4)-endoxylanases belonged to the glycoside hydrolase families (GH): 10 and 11 were found to be the most prevalent in xylanolytic fungi, with little GH5, GH8, andGH30 xylanases [10]. GH10 and GH11 xylanases have endo-acting manner but show different substrate specificity with respect to the substituent (MeGlcA or arbinofuranose) position, ability to cleave glycosidic linkage to MeGlcA or arbinosefuranose-substituted xylose residue, and numbers of unsubstituted xylose residues [2,11]. However, these two xylanase families can attack all types of xylans, reflecting the cleavage of xylan backbone is important. However, high substitution of the xylan backbones such as those found in corn fiber xylan impedes the hydrolyzing performance of GH10 and GH11 xylanases.

Plant pathogenic fungi have evolved to secrete a diverse arsenal of cell wall–degrading enzymes that enable them to overcome the structural barriers and defense systems of their hosts [12]. These enzymes not only facilitate nutrient acquisition but also play central roles in virulence, making them a rich source of unique cell-wall degradaing enzymes. Among them, xylanases are particularly significant. Beyond their nutritional function, xylanases contribute directly to pathogenicity, as evidenced by proteomic analyses and enzyme activity assays that reveal their abundant secretion during fungal growth on plant biomass [13]. Genetic studies further highlight their importance; for instance, silencing of the *Xyl1* gene markedly reduces fungal virulence, underscoring the role of xylanases in disease development [14,15] .

Fusarium species exemplify this strategy, producing a broad repertoire of xylanases capable of degrading plant cell walls and facilitating host colonization [16]. Several cases illustrate this enzymatic capacity. *Fusarium graminearum* Schwabe secretes two endoxylanases with high activity [17]. Similarly, *F. heterosporum* demonstrates strong xylanase activity when grown on barley-brewing residues under solid-state fermentation [18]. Other species, including *F. proliferatum* NRRL 26517 [19] and *F. oxysporum* f. sp. *cubense* [20], also display pronounced xylanolytic potential, highlighting the evolutionary advantage these enzymes confer in plant–fungus interactions.

Previous work in our laboratory reported the isolation of a novel strain, *Fusarium proliferatum* PSA-3, from mango leaves. This strain demonstrates the ability to grow efficiently on plant biomass and secrete large quantities of xylanase [21]. Members of the genus *Fusarium* are widely recognized as plant pathogens, causing diverse diseases such as wilts, rots, and dieback. Several species have also been implicated in leaf spot diseases, including severe outbreaks on mango leaves in regions such as Nigeria, Malaysia, and China [22]. A central determinant of pathogenicity in these fungi is their capacity to deploy cell wall–degrading enzymes, with xylanases serving as one of the key virulence factors [23,24].

Despite the importance of this enzymatic arsenal, the xylanolytic system of *F. proliferatum* PSA-3 remains poorly understood. Elucidating how this strain utilizes its complement of xylanases to

 doi:10.20944/preprints202509.2067.v1

attack plant cell wall polysaccharides is essential for understanding its infection strategies. In the present study, the xylanolytic enzyme system of *F. proliferatum*PSA-3 is characterized for the first time. Remarkably, these enzymes form aggregate-like multiprotein complexes in their intrinsic state. The resulting xylanolytic aggregates exhibit broad substrate specificity, efficiently degrading substrates ranging from simple xylo-oligomers to structurally complex glucuronoarabinoxylans and highly substituted arabinoxylans. These findings provide new insight into the enzymatic mechanisms employed by *F. proliferatum* PSA-3 to breach the highly intricate architecture of plant cell walls, which have evolved as natural barriers against microbial invasion. The work highlights the co-evolutionary dynamics between plants and pathogens and underscores the pivotal role of multiprotein enzyme assemblies in fungal virulence. A deeper understanding of the xylanolytic machinery of *F. proliferatum* PSA-3 may ultimately inform the development of innovative biocontrol strategies to support sustainable agriculture.

2. Results

Rice straw is a renewable lignocellulosic material that could serve as a feedstock in the production of biofuels and biochemicals in Thailand and other Asian countries. Also, rice straw was found to be a good growth substrate that induced protein secretion in *F. proliferatum* PSA-3 with high xylanolytic activity, surpassing other tested biomasses like Napier grass, cassava pulp, and durian peel (unpublished data). In addition, the critical involvement of xylanase activity in plant infection and penetration of plant cell walls during pathogenesis highlights the importance of learning about *Fusarium* spp. xylanase enzymes. Unfortunately, there is currently only a small amount of data available on the xylanolytic enzymes of pathogenic *F. proliferatum* species. To better understand the xylanolytic system of *F. proliferatum* PSA-3, we decided to cultivate the strain in rice straw.

2.1. Enzyme Production by Solid-State Fermentation

F. proliferatum PSA-3 was grown on rice straw for 12 days under solid-state fermentation, and the protein concentration and enzymatic activities in the crude protein extract at interval time were determined in this study (Figure 1). We found that the protein concentration increased dramatically from day 0 to day 7 (0.41±0.01 mg/mL corresponding to a total protein of 99.28±2.56 mg) and then remained constant. The xylanase activity against RAX (RAXase activity) increased rapidly from day 0 to 4, gradually increased until day 7, and then declined on day 12, whereas the xylanase activity against BWX (BWXase activity) increased rapidly from day 2 to 6 and then gradually declined. Herein, we also determined the activity against CMC (CMCase activity) as it has been reported that cellulase activity was co-expressed with xylanase in some *Fusarium* species [13,25,26]. We found that CMCase activity increased steadily from day 0 to day 9 and then decreased slightly. The highest enzymatic activity of BWXase, RAXase, and CMCase were observe on day 7, corresponding to 0.23±0.03 U/mL (56.85 U), 0.21±0.03 U/mL (50.22 U), and 0.10±0.01 U/mL (24.50 U), respectively. Based on these findings, *F. proliferatum* PSA-3 is a potent xylanase producing fungus and represents a good source of xylanolytic enzymes with low cellulase activity. Fungal xylanolytic and cellulolytic enzymes have been linked to growth, and the enzymes are secreted into the environment to break down high molecular weight polymers like xylan and cellulose before sugar assimilation. Our findings are consistent with other studies in terms of protein secretion, which increased over time and remained constant when the cells entered stationary phase, as well as xylanolytic and cellulolytic activity, which was commonly high during exponential growth phases and remained stable afterwards [27,28].

 doi:10.20944/preprints202509.2067.v1

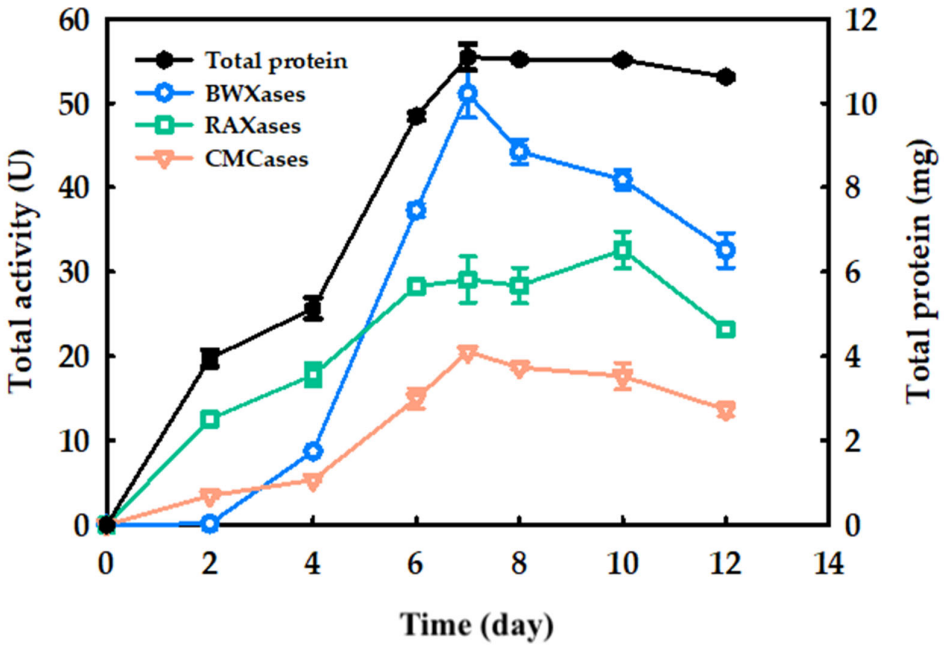

Figure 1. Time course profile of RAXase, BWXase, CMCase, and protein productions under solid state fermentation by *F. proliferatum* PSA-3 cultivated on rice straw at 28 ± 2 ºC.

2.2. Partial Purification of Xylanase

The xylanolytic enzyme system was investigated by extracting crude protein from a 7-day old culture of *F. proliferatum* PSA-3 cultivated on rice straw. The crude enzyme was partially purified by ammonium sulfate precipitation (85% saturation) and anion-exchange chromatography at room temperature (28 ± 2 ºC). The purification steps and enzymatic activity against RAX are shown in Table 1.

Table 1. Purification of xylanases from *F. proliferatum* PSA-3 during growth on rice straw.

Purification step	Volume (mL)	Protein concentration (mg/mL)	Enzyme activity (U/mL)	Total protein (mg)	Total activity (U)	Specific activity (U/mg)	Yield (%)	Purification (fold)
Crude enzyme	242	0.41±0.01	3.79±0.11	99.28±3.14	917.21±27.63	9.24±0.28	100	1
$(NH_4)_2SO_4$ precipitation	45	0.74±0.01	9.15±0.40	33.46±0.44	411.84±18.15	12.37±0.55	44.90	1.33
DEAE sepharose	1	0.16±0.02	25.04±3.03	0.16±0.02	25.04±3.03	156.47±18.94	2.72	17.19

A total of 45% of the protein was recovered after ammonium sulfate precipitation. Although this salting-out step reduced the overall protein yield by half, it was essential for removing brownish pigments from the crude extract, thereby minimizing interference in subsequent chromatographic purification. The enzyme preparation was then subjected to DEAE-Sepharose ion-exchange chromatography, which resolved two distinct activity peaks, designated as Peak I and Peak II (Figure 2), both exhibiting RAXase activity.

 doi:10.20944/preprints202509.2067.v1

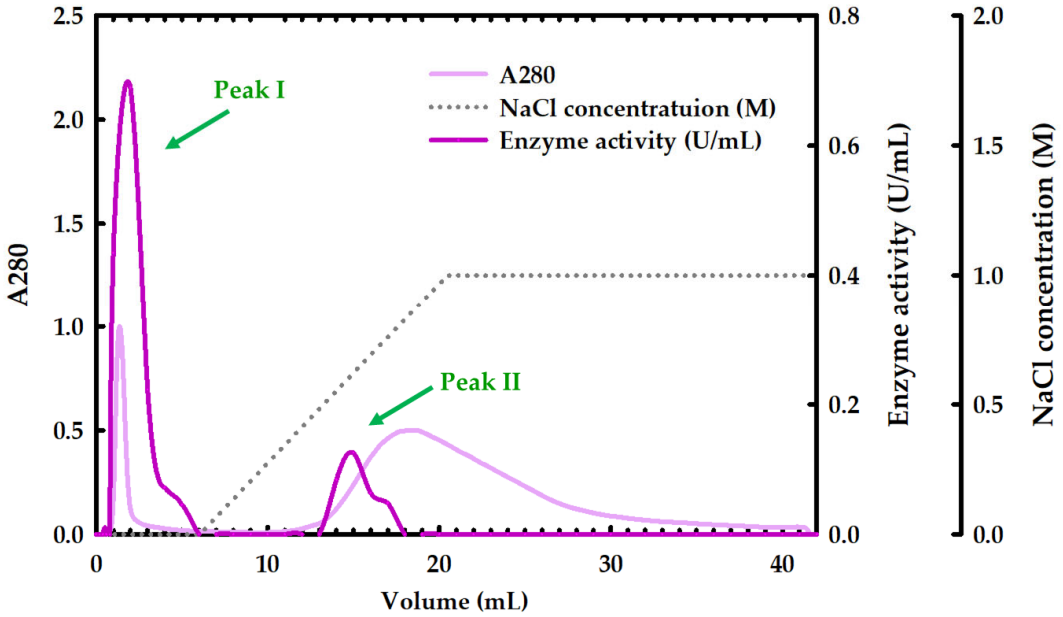

Figure 2. Chromatogram of purified xylanases separated by weak anion chromatography on Hitrap™ DEAE Sepharose FF 1 mL column with flow rate 0.75 mL/min.

It was observed that peak I was eluted at Fractions 1-3 without any added salt, but peak II was eluted at higher salt concentrations (Figure 2). The abrupt elution of peak I suggests that the protein was unable to form a stable interaction with the column. Here, we explored raising the pH of the binding buffer to 8.0 and employing a low ionic strength to increase the proteins' negative charges and decrease protein-salt competition for the resin binding sites. The peak I protein, however, continued to show no binding to the column. Peak I was chosen for this investigation because it had much higher RAXase activity (156.4718.94 U/mg) than Peak II (72.968.25 U/mg). Specific activity against RAX was 156.4718.94 U/mg, and overall protein recovery from peak I was 2.72%.

2.3. Gel Electrophoresis and Zymogram

The purified enzyme sample was subjected to both SDS-PAGE and active-PAGE analysis under varying conditions to shed light on the protein nature of peak I and the enzymatic activity. In this experiment, we studied the effects of SDS and a reducing agent on the protein by mixing the sample with either a Native-loading buffer (consisting of only dye and glycerol) or an SDS loading buffer (consisting of SDS and β-mercaptoethanol). The samples were introduced into the gel without heating it. We found that proteins loaded with either Native or SDS loading buffer showed no migration, as evidenced by the presence of the smear band at the top of the gel (Figure 3A, Lanes 1 and 2). Proteins are highly unlikely to move possibly because of their massive size, charges, and unfolding. Nevertheless, the protein showed activity against BWX and RAX (Figure 3B,C, Lanes 1 and 2).

 doi:10.20944/preprints202509.2067.v1

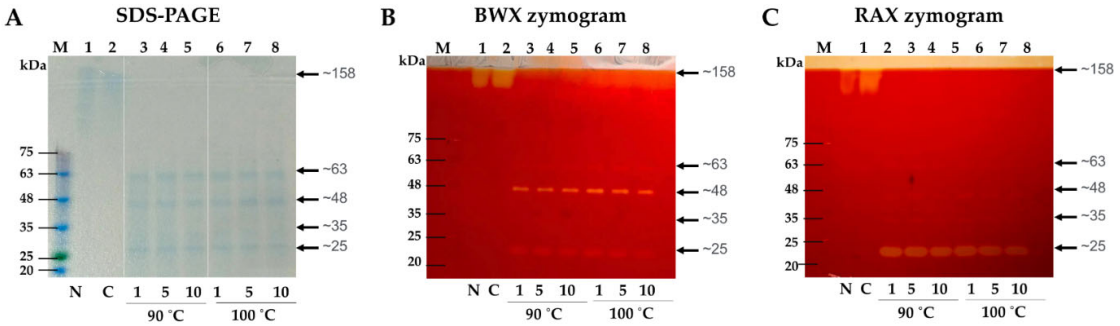

Figure 3. (**A**) SDS-PAGE analysis of purified xylanases, (**B**) Active-PAGE contained beechwood xylan, (**C**) Active-PAGE contained rye arabinoxylan. Lane M; protein molecular weight marker. Lane 1; sample mixed with Native dye (N). Lane 2; samples mixed with SDS loading buffer (no boiling) (S). Lanes 3, 4, and 5; sample mixed with SDS loading buffer treated at 90˚C for 1, 5, and 10 min, respectively. Lanes 6, 7, and 8; enzyme mixed with SDS loading buffer treated at 100˚C for 1, 5, and 10 min, respectively.

To explore protein stability and activity further, peak I protein was heat-treated in the presence of SDS loading buffer. The sample was treated at two temperatures: 90 and 100 ˚C, with incubation times ranging from 1 to 10 min. Heat treatment at 90 and 100 ˚C for 1 to 10 min broke down peak I protein into multiple smaller protein fragments (Figure 3A, Lanes 3-8), and at least four protein bands with sizes of approximately 25, 35, 45, and 63 kDa showed activity against BWX and RAX (Figure 3B,C). Based on the intensity of clear bands corresponding to enzymatic activity against red backgrounds, proteins with sizes of 63 and 35 kDa showed weak transparent bands on zymograms containing either BWX or RAX. The protein band with a size of 48 kDa was substantially more transparent against BWX than RAX. In contrast, the protein band with a size of 25 kDa showed more clearance on the RAX zymogram than the BWX zymogram. These findings suggested that the four proteins are distinct enzymes due to their sizes and activities.

We anticipated that the intact form of peak I protein appears as a high molecular weight aggregated protein with numerous xylanases with diverse modes of action based on the findings above. If this is correct, in gel-filtration chromatography, one peak should be present after peak I is applied. As expected, one broad peak with RAX activity occurred about 158 kDa (Figure 4). The occurrence of a greater molecular weight protein peak than individual proteins suggests that these protein components combine in their natural state. Therefore, peak I was considered xylanase aggregate and was further biochemically characterized in this study.

 doi:10.20944/preprints202509.2067.v1

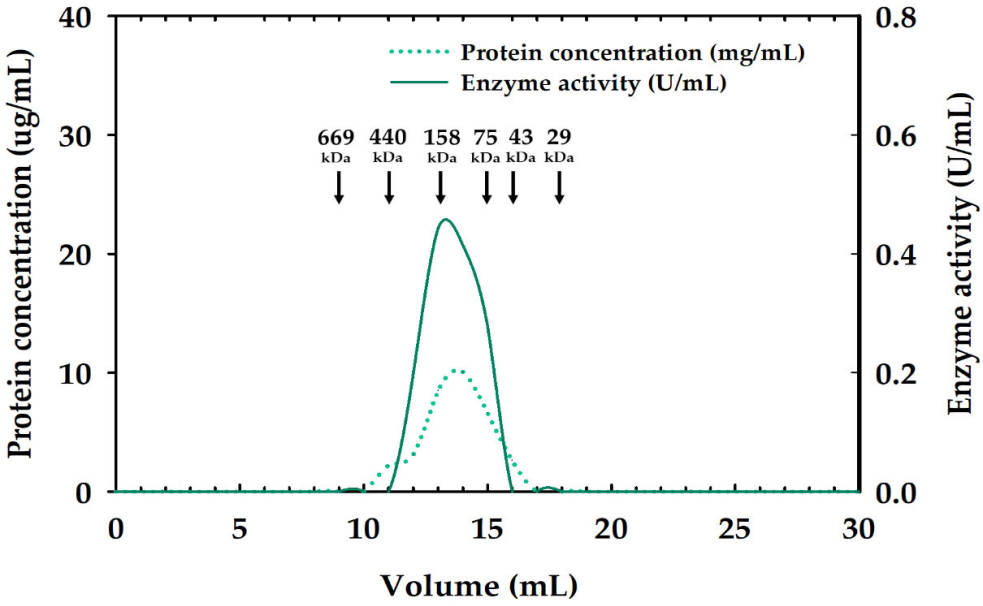

Figure 4. Gel-filtration chromatogram of peak I protein analyzed by a Superdex TM 200 Increase 10/300 GL column with a flow rate of 0.75 mL/min. Protein markers are denoted with arrows: Blue dextran (2,200 kDa, void volume), Thyroglobulin (669 kDa), Ferritin (440 kDa), Aldolasae (158 kDa), Conoalbumin (75 kDa), Ovalbumin (43 kDa), and Carbonic anhydrase (29 kDa).

2.4. Substrate Preference

The xylanase aggregate was tested for its hydrolyzing capability towards difference kinds of xylan (i.e., RAX, sWAX, iWAX, and BWX) and cellulosic (i.e., CMC and Avicel) substrates (Table 2). These substrates are β-glycosidic-linked xylose and glucose polymers. We found that the xylanase aggregate showed strong activity against RAX (156.47±18.94 U/mg), followed by sWAX (110.28±2.73 U/mg) and BWX (63.42±1.69 U/mg). The slight activity was observed with iWAX (31.31±2.59 U/mg) and CMC (41.86±1.41 U/mg), respectively and exhibited no activity against Avicel. These results suggested that xylanolytic activity is the main activity of the enzyme aggregate based on the greater hydrolyzing performance towards a variety of xylans than cellulose, and the inability to degrade Avicel confirms that insoluble crystalline cellulose is not a preferred substrate for the enzyme. Compared to the activity against RAX, the four-time lower activity against CMC suggested that CMCase is a side activity of the xylanase aggregate. The occurrence of side activity is possible because CMC shares some properties with xylan in terms of chemical bonding and structural similarities. Furthermore, due to its high solubility, CMC is easily accessible to the active sites of the enzyme.

Table 2. Quantification of enzymactic activity of xylanase aggregate.

Substrate	Total activity (U)	Specificity (U/mg)
Rye arabinoxylan (RAX)	25.04±3.03	156.47±18.94
Soluble wheat arabinoxylan (sWAX)	17.65±0.44	110.28±2.73
Insoluble wheat arabinoxylan (iWAX)	5.01±0.41	31.31±2.59
Beechwood xylan (BWX)	10.15±0.27	63.42±1.69
Carboxymethyl cellulose (CMC)	6.59±0.22	41.86±1.41
Microcrystalline cellulose (Avicel)	0.00±0.00	0.00±0.00

 doi:10.20944/preprints202509.2067.v1

2.5. Biochemical Characterization of Xylanase Aggregate

In the following study, we chose RAX and BWX as the xylan substrates with high and low arabinose substitution to determine the property and working nature of xylanase aggregate towards the complex xylans.

2.5.1. Effect of pH and Stability

The optimal pHs were determined using RAX and BWX as the substrates (Figure 5A,B). We found that the aggreated xylnase were active from pH 3.0 to 9.0 against both RAX amd BWX. The maximal pHs of RAXase and BWXase acivities were 5.0, and more than 80% of maxium activity of RAXase and BWXase were 4.0-7.0 and 5.0-8.0, repectively. The slight differece in the pH range for degrading RAX and BWX is possibly due to the fact that the xylanase aggregate contians multiple xylnases that migh have had diffeent working pHs.

The pH stability of the agregrated xylanase was studied by preincubating the enzyme in the buffers with different pHs for 1 h prior to determining the residual activity of the enzyme against RAX and BWX. We found that the RAXase activity of aggregated xylanase retained more than 80% residual activity in the pH range from 4.0 to 8.0 (Figure 5C), while the BWXases reteaine more 80% residual activty from pH 5.0-8.0 (Figure 5D).

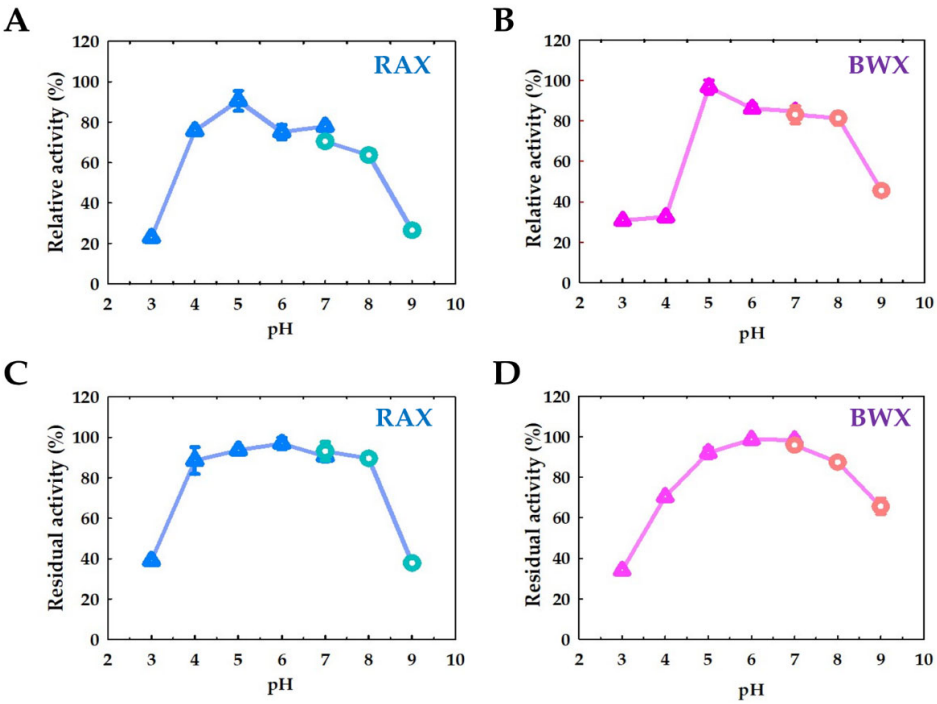

Figure 5. Effect of pH on xylanolytic activity against RAX (A) and BWX (B) of the aggregated xylanase. pH stability of aggregate xylanase against RAX (C) and BWX (D). Citrate buffer △ and Tris-HCl bufffer (○).

2.5.2. Effect of Temperature and Stability

The effefct of temperatures on aggreagted xylanase acivity against RAX and BWX were determined in the temperature range of 20˚C to 80 ˚C. We found that the maximal temperature of RAXases and BWXases was 50˚C (Figure 6A,B). The RAXases retained more than 60% activity at 40 ˚C and 50% activty at 50˚C, for 2 h (Figure 6C), while, BWXases retained more 70% activity at 40 ˚C for 2 h, and rapaidly decreased at 50˚C (Figure 5D).

 doi:10.20944/preprints202509.2067.v1

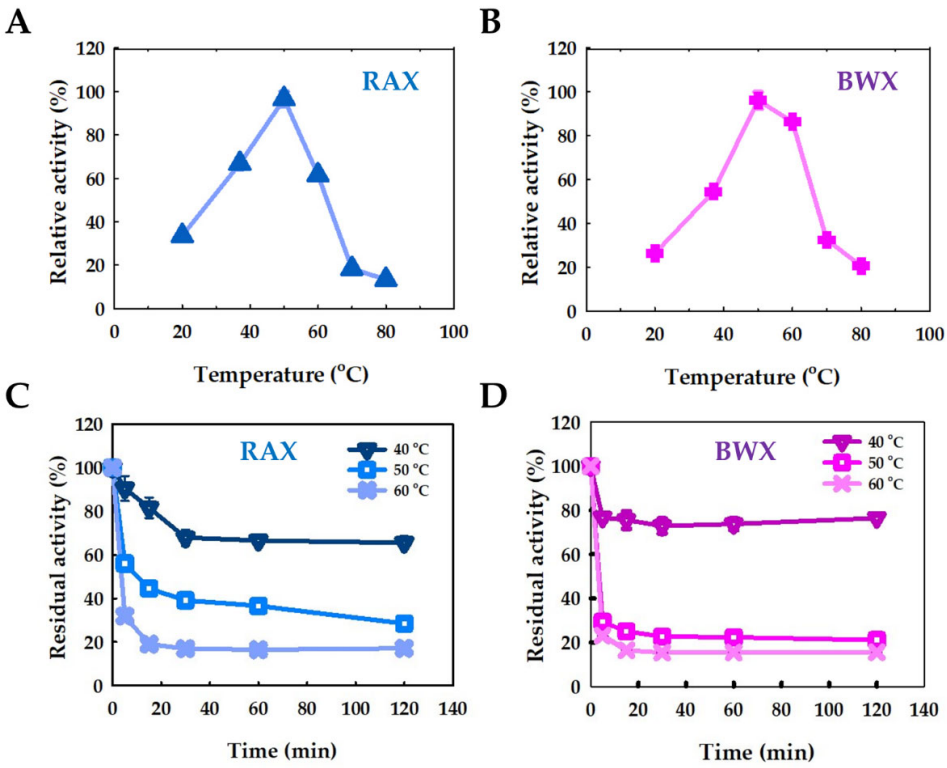

Figure 6. Effect of temperature on xylanaloytic activity against RAX(A) and BWX (B) by the aggregated xylanase. Thermal stability of the aggregated xylanase activity against RAX (C) and BWX (D).

2.5.3. Effect of Metal Ion and Chemical Reagent

Enzyme activity can be affected both positively and adversely by different metal ions and chemical reagents. In the presence of metal ions and chemical reagents, the hydrolysis of RAX and BWX by xylanase aggregate was investigated to see how the xylanolytic activity was affected. We found that, at the concentrations of 1 mM and 10 mM, EDTA, Ca^{2+}, Mg^{2+}, Co^{2+} slightly reduced the RAXase and BWXase activities (Figure 7A,B). Moreover, 10 mM Cu^{2+} significantly reduced RAXases (64%) and BWXase (47%) activities, repectively. At a concentration of 10 mM, Ni^{2+} and Fe^{2+} slightly increased RAXase activity by 20% and 13%, respectively; whereas 1 mM Co^{2+} and 10 mM Fe^{2+} increased BWXase activity by 7% and 11%, respectively.

 doi:10.20944/preprints202509.2067.v1

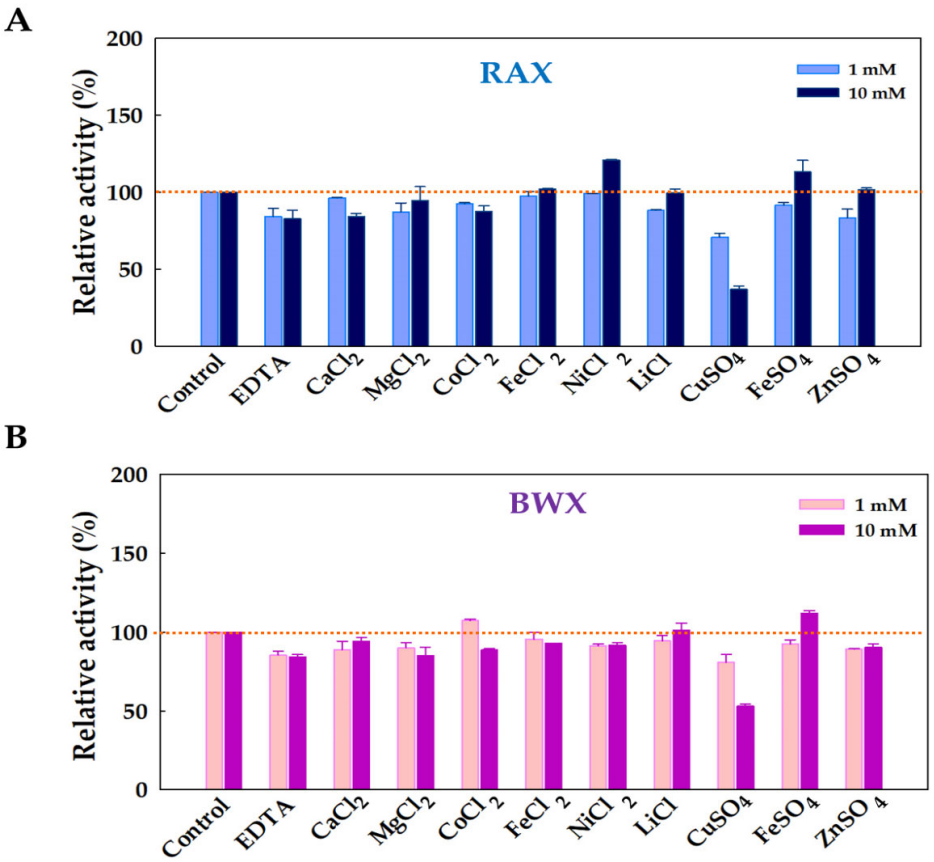

Figure 7. Effect of metal ion with PSA-3 xylanase.

From Table 3, it was observed that Tween-20 and Tween-80 at the concentrations of 1% and 5% (v/v) increased approximately 8-30% activty for RAXase and BWXase. At 5% (v/v), Triton X-100 reduced RAXase activity by about 30% but slightly decreased BWAXase activity nore more than 55%. SDS significantly reduced RAXase and BWXase activities by around 50% and 40% at a comcentration of 5 mM. β-mercaptoethanol increased BWXases activity by 7%, but decreased RAXase activity by 20%.

Table 3. Effect of different chemical reagents on xylanolytic activity against RAX and BWX by xylanase aggregate.

Compounds	Relative activity (%) of RAXase		Relative activity (%) of BWXase	
	1%	5%	1%	5%
Tween-20	108.78±2.66	126.96±3.37	115.61±1.68	130.16±3.62
Tween-80	96.34±4.73	117.09±6.13	117.73±2.22	118.86±1.40
Triton X-100	83.46±3.83	77.00±8.58	97.45±1.91	94.83±5.49
SDS	73.45±3.17	53.41±0.19	71.56±2.33	61.48±1.77
	2mM	5 mM	2mM	5 mM
β-mercaptoethanol	80.23±0.31	80.65±1.72	107.09±4.10	106.78±1.65

 doi:10.20944/preprints202509.2067.v1

2.6. Kinetic Parameters of Xylanase Aggregate

Despite the fact that the xylanase aggregate contained multiple xylanases, we opted to determine the kinetic parameters to understand how the entire xylanases work on the given complicated xylan substrates and determined the rate of substrate association to anticipate the enzyme performance. We found that the xylanase aggregate acted differently towards RAX, sWAX, and BWX (Figure 8). K_m and V_{max} values for the hydrolysis of RAX were 6.26 mg/mL and 0.87 mM/min, respectively (Figure 8A), whereas the values for sWAX were 9.91 mg/mL and 1.07 mM/min, respectively (Figure 8B). The K_m and V_{max} values for BWX hydrolysis were 18.26 mg/mL and 0.68 mM/min, respectively (Figure 8C). It was observed that K_m, an indicator of the enzyme's binding affinity for its substrate, was found to be lowest for the RAX hydrolysis, suggesting that the enzyme is more effective at hydrolyzing RAX than sWAX and BWX at lower substrate concentrations. The maximum rate of hydrolysis (V_{max}) of sWAX, however, was somewhat higher than that of RAX. RAX is quite viscous, thus we reasoned that vicosity might influence the rate with which its hydrolysis reaction proceeds. Among others, the high K_m and low V_{max} values were observed in the hydrolysis of BWX, which contains very few arabinose substituents.

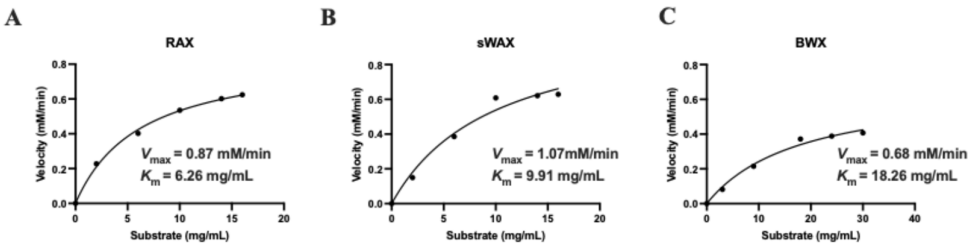

Figure 8. Kinetics parameters (K_m and V_{max} values) of xylanase aggregate against RAX, sWAX, and BWX.

2.7. Time Course of Enzymatic Hydrolysis and Analysis of Hydrolysis Products

We next investigated the profile of xylan and related substrate hydrolysis by the xylanase aggregate and determined the hydrolysis products. In this study, three types of substrates were used: model polysaccharide xylans (RAX, sWAX, iWAX, and BWX), extracted xylans from sugarcane bagasse and Napier grass, and unbranched and branched xylo-oligosaccharides.

We found that the hydrolysis of RAX, sWAX, iWAX, and BWX by the xylanase aggregate produced reducing sugar at different degrees (Figure 9A). The release of reducing sugars from RAX and sWAX increased rapidly from 0 to 5 min, then gradually increased from 15 to 60 min, and remained constant after 60 min. The maximum reducing sugar yields for RAX and sWAX were 4440.12±45.51 μg/mL and 3705.09±149.40 μg/mL, respectively. During BWX hydrolysis, the release of reducing sugar increased with time, reaching its maximum yield of 4127.84±48.80 μg/mL after 120 min. The release of reducing sugar from iWAX slightly increased from 0 to 30 min and then remained steady, providing a reducing sugar concentration of 733.38±23.26 μg/mL.

We then qualitatively analyzed the hydrolysis products from RAX, sWAX, iWAX, and BWX at various time intervals using TLC technique. We found that, from all substrates tested, a series of xylo-oligosaccharides were generated, and the accomulation of short oligosaccharides increased with time (Figure 9B–E). Xylobiose (X2) and Xylotriose (X3) appeared to be the major hydrolysis products followed by larger oligomers such as xylotetraose (X4) and xylopentaose (X5) and a very few xylohexaose (X6). In addtion, we oberved that some oligomers produced did not match the sugar standards (Figure 9B–E). We speculated that those oligomers were branched xylo-oligosaccahrides because the xylan substrates contain either arbinoses or glucuronic acids as substiuents on the xylan backbones.

 doi:10.20944/preprints202509.2067.v1

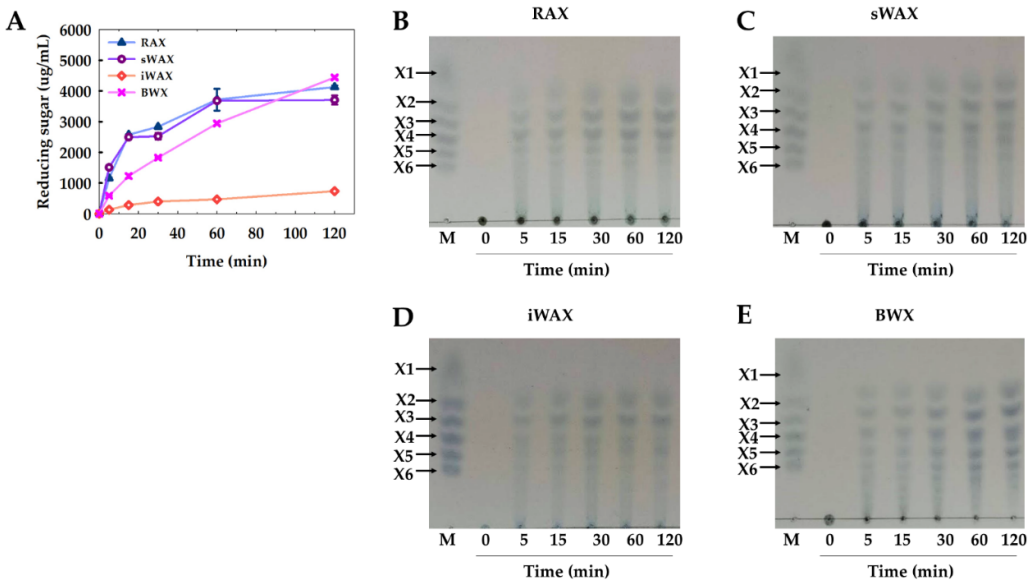

Figure 9. Release of reducing sugar from pure polysaccharides by xylanase aggregate (A) and and TLC analysis of hydrolysis products from RAX (B), sWAX (C), iWAX (D), and BWX (E). M, standards of xylose and xylo-oligosaccharides with a degree of polymerization of 2-6 (X2-X6).

For hydrolysis of extracted xylans from sugarcane bagasse and Napier grass, the release of reducing sugars by aggregate xylanase varied (Figure 10A). The release of reducing sugars from both sugarcane bagasse and Napier grass xylans was observed to increase rapidly from 0 to 60 min and then to slowly increase thereafter, with the production rate of sugarcane bagasse xylan being higher than that of Napier grass xylan. At 120 min of incubution, the release of reducing sugars for sugarcane bagasse xylan (1759.12±44.51 μg/mL) was about two-time higher than Napier grass xylans (829.86±0.56 μg/mL). TLC analysis reveals that the primary hydrolysis products obtained from sugarcane bagasse and Napier grass xylans were very comparable, with X2-X4 being the most abundant (Figure 10B,C). These findings suggest that xylanase agregate cleaves both xylans at the same sites, and the variation in reducing sugar yields may be attributable to differences in substrate solubility.

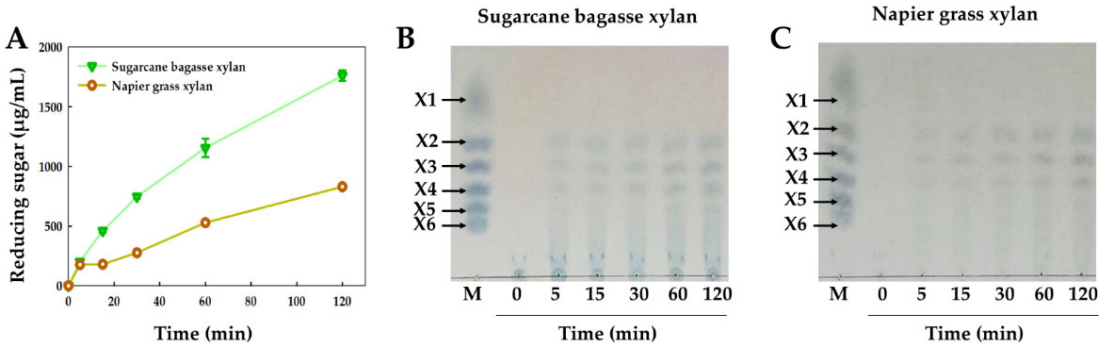

Figure 10. Release of reducing sugar from sugarcane bagasse and Napier grass xylans by xylanase aggregate (A) and TLC analysis of hydrolysis products from sugarcane bagasse (B) and Napier grass (C) xylans. M, standards of xylose and xylo-oligosaccharides with a degree of polymerization of 2-6 (X2-X6).

 doi:10.20944/preprints202509.2067.v1

2.8. Modes of Action

We analyzed hydrolysis cleavage of the xylo-oligosaccharide to get insight into the xylanase agregate's cleavage mechanism. In this case, the unbranched oligomers X2-X6 served as substrates. We found that X6 was completely converted to X2, X3, and X4 within 1 min, while X5 was gradually hydrolyzed to X2 and X3, with complete hydrolysis of X5 to X2 and X3 occurring within 30 min (Figure 11). The hydrolysis of X4 to X2 was observed at 1 min and the conversion of X4 to X2 increased with time. However, by 30 min, X4 remained, indicating that the rate at which X4 could be converted to X2 was slow. Under assayed conditions, X2 and X3 were not hydrolyzed by the xylanase aggregate (Figure 11). The rapid hydrolysis of X6, followed by X5 and X4, suggests that the xylanase aggregate prefers hydriolyzing xylo-oligosaccharides with a degree of polymerization greater than four. The inability to hydrolyze X2 and X3 indicate that they are final products.

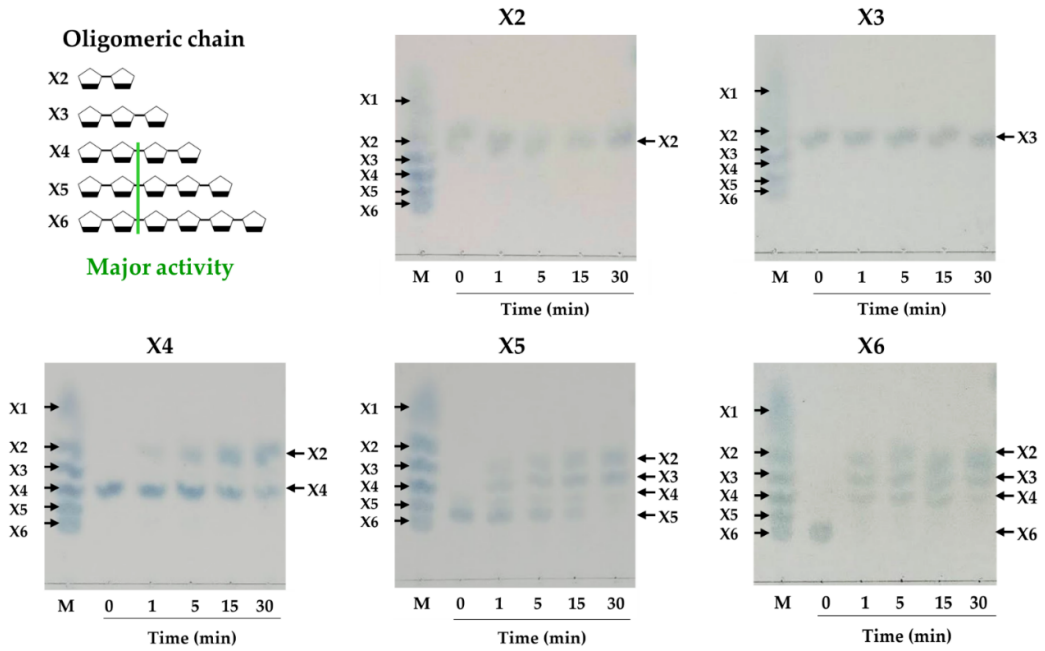

Figure 11. TLC analysis of hydrolysis products from xylo-oligosaccharides (X2-X6) by xylanase aggregate at various times. M, standards of xylose and xylo-oligosaccharides with a degree of polymerization of 2-6 (X2-X6).

Next, we seek to know more about the mechanism by which xylanase aggregate act on substitued xylans. In arabinoxylan, O-2 and O-3 positions of the β-(1-4)-linked xylopyranosyl backbone can be mono- or disubstituted with α-L-arabinofuranose [29]. Therefore, its enzymatic activity was evaluated using the model branched xylo-oligosaccharides, namely 2^3-α-L-arabinofuranosyl-xylotriose (A^2XX) , $2^3,3^3$-di-α-L-Arabinofuranosyl-xylotriose ($A^{2,3}XX$), and 3^3-α-L-arabinofuranosyl-xylobiose (A^3X).

We found that the xylanase aggregate did not hydrolyze the substrates A^2XX, $A^{2,3}XX$, and A^3X within 30 min. However, with a longer incubation time of 19 h (overnight), A^2XX, $A^{2,3}XX$ were slightly degraded, while A^3X remained unchanged (Figure 12). It was noticed that the both mono- and disubstitued substrates that contained arabinose substituents at O-2 poositions was degraded, suggesting the ability of the enzyme to hydrolyze α-(1,2)-L-arabinofuranosidic linkages in the branched arabinoxylan. Moreover, after 1-h incubation, very neglegible activity was detected against p-nitrophenyl arabinofuranoside, a synthetic substrate typically employed to test for arabinofuranosidase activity. Due to their slow hydrolysis rate, substituents on xylans are resistant to breakdown by xylanase aggregate.

 doi:10.20944/preprints202509.2067.v1

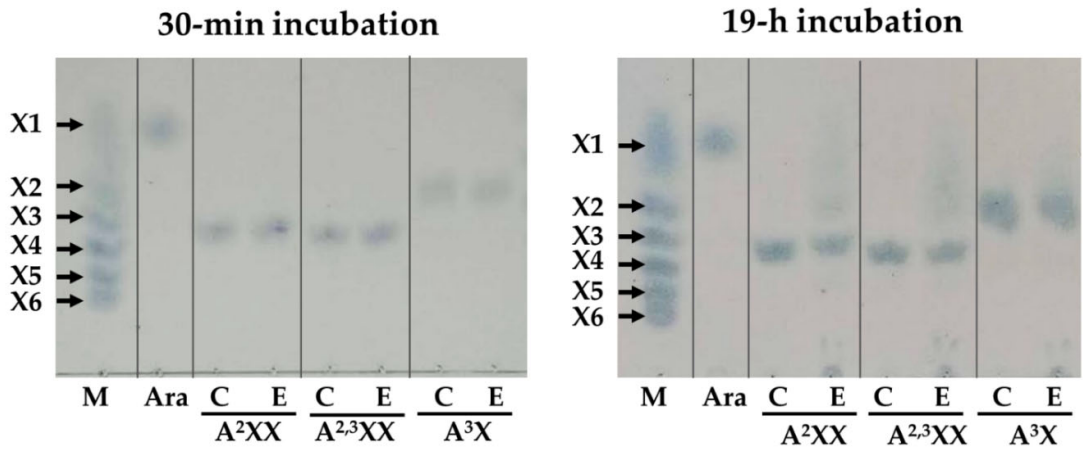

Figure 12. TLC analysis of hydrolysis products by xylanase agrregate using branched xylo-oligosacchraides: A^2XX, $A^{2,3}XX$, and A^3X as the substrates. The incubation times were 30 min and 19 h. M, standards of xylose and xylo-oligosaccharides with a degree of polymerization of 2-6 (X2-X6). Ara, standard of arabinose. The letter C stands for the reaction control, which includes denatured enzyme and substrate. The letter E stands for enzymatic reaction, which includes both enzyme and substrate.

3. Discussion

The plant cell wall functions as a primary physical barrier, forming the first line of defense against environmental stress and microbial attack. To overcome this barrier, plant pathogens secrete suites of extracellular cell wall–degrading enzymes that act as virulence factors during infection [30]. Enzymes such as pectate lyases, polygalacturonases, cellulases, β-glucosidases, and xylanases have all been implicated in the direct degradation of host cell walls [31–33].

Within this context, *Fusarium* species are notorious plant pathogens responsible for a wide range of economically important crop diseases. *Fusarium proliferatum*, in particular, has been reported as a causal agent of diseases in tomato, pumpkin, banana, soybean, wheat, sugarcane, maize, and rice [31,32,34–36]. It has also been associated with leaf spot disease in mango, whose leaves can contain up to 54% dry weight in structural polysaccharides [37]. Although the precise mechanisms by which *F. proliferatum* circumvents host defenses remain incompletely understood, several studies indicate that the fungus penetrates host tissue by secreting a combination of pectinases, cellulases, and xylanases to breach the cell wall barrier [34].

Because the cell walls of major crops such as sugarcane, maize, barley, and rice are particularly rich in cellulose and xylan, it is unsurprising that *F. proliferatum* produces both cellulases and highly active xylanases during infection, with xylanase secretion being especially prominent ([36,38]. These enzymes soften host cell walls, thereby facilitating invasion and nutrient uptake. Understanding the xylanolytic system of *F. proliferatum* is therefore essential for elucidating the molecular basis of host–pathogen interactions and may also reveal opportunities for harnessing fungal xylanases in agricultural and biotechnological applications. To date, however, only a limited number of studies have investigated xylan-degrading enzymes in *F. proliferatum* [19,39,40]

In this study, we attempted to investigate and expand our understanding of the xylanolytic enzyme system of *F. proliferatum* PSA-3. Under solid state fermentation, we first cultured the fungus on rice straw, an abundant agricultural byproduct high in xylan (Figure 1). We discovered that *F. proliferatum* PSA-3 grew well on rice straw and had substantial xylanolytic activity against RAX and BWX. RAX and BWX are commonly used substrates to detect endo-β-(1,4)-xylanase activity, with RAX and BWX being arabinoxylan (arabinose: xylose = 38: 62) and glucuronoxylan (xylose: glucuronic acid: other sugars = 86.1: 11.3: 2.6) Within 2-day of cultivation, RAXase appeared to increase quickly, indicating that activity against arabinoxylan is important. The fast and relatively

 doi:10.20944/preprints202509.2067.v1

high production of RAXase at the early stage of the fungal growth may thus reflect the xylan in rice straw being present in arabinoxylan and arabinoglucuroxylan forms [41,42]. BWXase activity, together with CMCase activity, appeared to increase rapidly after 4-day of cultivation. Among the activities detected, BWXase activity was the greatest, followed by RAXase and CMCasxe activity. Our findings are similar to those *Humicula grisea* cultivated on sugarcane bagasse and *Aspergillus niger* cultivated on sugarcane bagasse and brewer spent grain for 5-7 days (log phase), with BWXase activity being the highest [27]. Furthermore, numerous *Fusarium* spp. are have been identified as hyper-productive xylanase strains [33,43–45], and the most peak enzyme production occurring during the exponential phase of growth [46].

The steady concentration of secreted protein, aligned with fungal growth, indicates that *F. proliferatum* PSA-3 entered the stationary phase after approximately seven days of incubation. Growth suppression at this stage is likely due to nutrient depletion, reduced water availability, and the accumulation of toxic metabolites during fermentation [47,48]. Enzyme activity profiles further reflected this shift in physiology. BWXase activity declined sharply, whereas CMCase activity showed only a modest reduction. The loss of activity may be explained by reduced enzyme stability or feedback inhibition caused by the buildup of hydrolysis byproducts during xylan and cellulose degradation.

In contrast, RAXase activity remained relatively stable throughout incubation. This persistence may reflect the enzyme's higher tolerance to end-product accumulation and inhibitory compounds, allowing sustained activity even under unfavorable fermentation conditions [49–51]. Such resilience toward arabinoxylan substrates could provide a selective advantage in natural environments where plants produce complex, highly substituted xylans as defense barriers. Collectively, these findings suggest that enzyme regulation in PSA-3 is substrate dependent, with RAXase displaying robustness that may contribute to the pathogen's ability to colonize arabinoxylan-rich plant tissues.

Two main protein peaks with xylanolytic activity against RAX were obtained from the crude extract of *F. proliferatum* PSA-3 culture by virtue of ammonium sulfate precipitation and anion-exchange chromatography (Figure 2). Peak I showed a relative higher RAXase activity than peak II and it existed as a high molecular wight xylanase containing aggregate (158 kDa), which was evidenced by gel filtration analysis and the dissociation of protein components under heat treatment in the presence of SDS and β-mercaptoethanol. The major four protein bands with sizes of 63, 48, 35, and 25 kDa showing distinct enzymatic activity against RAX and BWX proved the protein aggregate have various xylanases in its structure. In the previous work, the aerobic fungus *Chaetomium* sp. nov. MS-017 has shown to produce a massive multienzyme complex [52]. The enzyme complex with a molecular wight of 468 kDa contained at least five xylanases as well as cellulases and pectinases. It was proved to be multienzyme complex based on the dissociation of multiple proteins after being denatured without β-mercaptoethanol at 80 ºC for 5 min [52]. Some multiple xylanase complex referred to as xylanosome have been identified in xylanolytic bacteria that produces large to ultra-large structures varying in size ranging from 300 to 2000 kDa [53–56]. The features of those xylanolytic mutienzyme complex are strong interactions among protein components, requiring strong denaturing conditions (boiling in the presence of SDS and β-mercaptoethanol for 5 to 10 min) to completely separate individual polypeptides, and a signature high molecular weight, non-enzymatic protein serves as a scaffold to integrate several enzyme subunits into the complex [55–58]. In contrast to xylanosome or a discrete multienzyme complex cellulosome assembled though high affinity protein-protein interaction [59], the peak I was assumed to be xylanase aggregate in our study because the interaction between polypeptides appeared to be more easily broken down into fragments, which is evidenced by the dissociation of protein components with the relatively short heat treatment (1 min for 90 °C). The main interaction of the xylanase aggregate could involve non-specific charged-charged and electrostatic interactions. In addition, no high molecular weight proteins can be assumed to be a scaffolding protein based on SDS-PAGE results. Recently, some studies have demonstrated that *Cellulosimicrobium cellulans* might use a new way to assemble proteins into complex by combining monomeric proteins with mono- or bifunctional activity to form compact

 doi:10.20944/preprints202509.2067.v1

folding structure that is stabilized by calcium [60–62]. Moreover, a few xylanases have been found to contain more than one polypeptide. The xylanase from *Thermoanaerobacterium* sp. strain JW/SL-YS485 xylanase was made up of two heterosubunits of 180 and 24 kDa, both of which have xylanase activity [58,63]. Nevertheless, without heat treatment, the xylanase aggregate showed good resistance to SDS and β-mercaptoethanol because the protein exists in the aggregate form. Accordingly, although the assembly of the protein and relationship of active protein components are not clearly elucidated on the present study, we believe that the incorporation of xylanase into the aggregate may be advantageous in terms of improved tolerance to chemicals or solvents and spatial proximity effects [61], and the reason why RAXase activity was functionally active and quite stable throughout the growth of *F. proliferatum* PSA-3 on rice straw may be due to the fact that RAXase activity is associated with xylanase aggregate formation.

The biochemical properties of *F. proliferatum* PSA-3 xylanase aggregate were studied to ascertain how environmental variables influence xylanolytic activity. We reported that both RAXase and BWXase activities of the xylanase aggregate were active in a wide pH range from 3.0 to 9.0, with activity greater than 80% from pH 4.0 to 8.0. This feature distinguishes it from most fungal xylanases, which have a narrow working pH range in acidic to neutral conditions. For example, with the activity more than 80%, the xylanase from *Trichoderma inhamatum* was active in pH ranges varying from 4.5 to 6.5 [64], and the xylanase from *Fusarium heterosporum* was active in pH ranges ranging from 4.5 to 5.5 [18]. We reasoned that the hydrolyzing capacity of the xylanase aggregate across a broad pH range from acid to alkaline conditions is a result of monomeric xylanases in its structure having varying pH optimum and stability. When testing the influence of temperature on xylanolytic activity, the xylanase aggregate demonstrated maximum RAXase and BWXase activities at 50 °C. It exhibited good thermal stability at 40 °C, retaining more than 80% activity against RAX and BWX over 2 h. Fungal xylanases typically prefer temperatures around 30 to 50 °C [65,66]. Although the activity immediately reduced when incubated at 60 °C, the half-life (5 min at 60 °C) of the xylanase aggregate against RAX and BWX was significantly longer than that of monomeric xylanase. For example, the half-lives of *Trichoderma inhamatum* xylanases I and II at 60 °C were 40 and 46 s, respectively [64]. Some microorganisms have shown that integrating enzymes into the complex is one strategy for improving the thermal stability of their enzymes [52,61].

The enzymatic activity of *F. proliferatum* PSA-3 xylanase aggregate against RAX and BWX was negligible affected by metal ions: Ca^{2+}, Mg^{2+}, Co^{2+}, Fe^{2+}, Ni^{2+}, Zn^{2+}, and Li^{2+} at 10 mM, except Cu^{2+}. Similar results have been observed in xylanolytic multienzyme complex from *Chaetomium* sp. nov. MS-017 [52] and *Tepidimicrobium xylanilyticum* [53]. The resistance to cations is possibly due to xylanase aggregate having enzyme components with good tolerance to cations. Moreover, the assembly of several enzymes into aggregate or complex is thought to relieve the adverse impact of cations on enzymatic activity [52,53]. However, Cu^{2+} has been found to be a strong inhibitor of xylanase activity.

The xylanolytic activity of the enzyme aggregate from *F. proliferatum* PSA-3 was only slightly affected by EDTA, whereas SDS strongly inhibited activity, and β-mercaptoethanol showed no significant effect (Table 3). These results suggest that intermolecular associations within the aggregate are stabilized primarily through hydrogen bonding rather than disulfide linkages [18]. Consequently, the xylanase aggregate remains stable in the presence of reducing agents but is disrupted by heat and SDS, which break hydrophobic interactions and hydrogen bonds in proteins [67].

The influence of thiol-containing compounds on xylanase activity appears to vary among fungi. For example, β-mercaptoethanol and dithiothreitol (DTT) enhanced the activity of xylanase from *F. heterosporum* by 55% and 54%, respectively [18]. Likewise, crude xylanases from *T. longibrachiatum* and *A. niger* were activated by L-cysteine, DTT, and β-mercaptoethanol [68]. These stimulatory effects may arise from the ability of reducing agents to prevent oxidative inactivation of the enzymes. Consistently, the activity of xylanase aggregate was also enhanced in the presence of non-ionic surfactants such as Tween-20 and Tween-80.

 doi:10.20944/preprints202509.2067.v1

Kinetic analysis revealed that the xylanase aggregate from *F. proliferatum* PSA-3 exhibited a clear preference for RAX and sWAX, two arabinoxylans with high levels of arabinose substitution (~40% and ~38%, respectively). The aggregate showed strong binding affinity for both substrates, with K_m values of 6.26 mg/mL for RAX and 9.91 mg/mL for sWAX, indicating that arabinose substitution on the xylan backbone does not hinder enzyme–substrate interaction. Interestingly, the V_{max} for sWAX (1.07 mM/min) was slightly higher than that for RAX (0.87 mM/min), a difference likely attributable to the higher viscosity of RAX, which may restrict substrate diffusion and mass transfer. By contrast, BWX, a glucuronoxylan substituted with 13% glucuronic acid, showed a relatively high K_m (18.26 mg/mL) and a lower V_{max} (0.68 mM/min), reflecting weaker binding affinity and reduced catalytic efficiency compared with RAX and sWAX. These findings differ from reports of other xylanase complexes that preferentially hydrolyze long-chain, less substituted xylans [52,55,56], likely due to steric requirements for substrate accessibility. In contrast, the PSA-3 xylanase aggregate displayed robust hydrolytic activity against highly substituted arabinoxylans, while retaining activity toward glucuronoxylans such as BWX. We propose that arabinose residues may serve as recognition elements for specific monomeric xylanases within the aggregate [69–72]. Supporting this hypothesis, zymogram analysis revealed a 25-kDa protein band exhibiting strong activity against RAX-incorporated gel (Figure 3). The strong activity of the enzyme aggregate against complex arabinoxylans may help explain why *Fusarium* species are frequently associated with diseases in cereal grains and mango leaves, which are naturally rich in arabinoxylans [22,73–75].

Hydrolysis of pure polysaccharides (BWX, RAX, sWAX, and iWAX) by the *F. proliferatum* PSA-3 xylanase aggregate yielded products ranging from X2 to X6 (Figure 9). In contrast, hydrolysis of extracted sugarcane xylan and Napier grass xylan produced only X2–X4 on the TLC plate (Figure 10). The difference in product profiles between pure polysaccharides and extracted xylans is likely due to the lower solubility and reduced accessibility of the latter, which limit enzymatic attack by the xylanase aggregate, as observed by the release of reducing sugars (Figures 9A and 10B). Compared with the action of monomeric xylanases, the PSA-3 aggregate displayed a distinct hydrolytic pattern. For instance, the xylanase from *F. proliferatum* NRRL 26517 generated mainly X2 from RAX and WAX [19], while *F. heterosporum* produced X2–X5 from birchwood xylan [18]. Similarly, the xylanosome complex from *Streptomyces olivaceoviridis* E86 released X2 and X3 as major products from BWX and X1–X3 plus arabinose from WAX [56]. The xylanosome of the thermophilic fungus *Chaetomium* sp. nov. MS-017 produced X2 and X3 as dominant products from oat spelt xylan, along with minor amounts of X1, X4, X5, and X6 [52]. Taken together, these observations suggest that the PSA-3 xylanase aggregate comprises multiple xylanase components, with endo-type enzymes likely dominating the activity. This inference is supported by the diverse series of oligosaccharides (X2–X6) generated during hydrolysis.

To investigate the mode of action of the PSA-3 xylanase agrreagate, xylo-oligosaccharides (X2–X6) were used as substrates. The enzyme aggregate showed no activity on (X2) or (X3), but readily hydrolyzed X4 and X5, and completely degraded X6 within 1 min at 37 °C (Figure 11). The accumulation of X2 and X3 during the hydrolysis of X5 and X6 is consistent with the enzyme's inability to cleave these shorter oligomers [52,56], indicating that X2 and X3 represent final products. These findings demonstrate that the major activity of the PSA-3 xylanase aggregate is directed toward longer-chain xylo-oligosaccharides, confirming its predominant endo-acting nature. This conclusion is further supported by hydrolysis studies with pure polysaccharides (BWX, RAX, sWAX, and iWAX) and extratced xylans (Figures 9 and 10), which yielded a series of products from X2 to X6. The incomplete hydrolysis of these polysaccharides may be attributable to product inhibition by the accumulating X2 and X3 [76].

We further examined the activity of the PSA-3 xylanase aggregate against highly substituted arabinoxylan oligosaccharides using A^2XX, $A^{2,3}XX$, and A^3X as substrates. No hydrolysis was detected within a short incubation period of 30 min. However, after prolonged incubation for 19 h, partial hydrolysis of A^2XX and $A^{2,3}XX$ was observed, while A^3X remained resistant. The slow catalytic rate may reflect the short chain length of these substrates, which likely prevents proper

 doi:10.20944/preprints202509.2067.v1

accommodation within the enzyme's binding sites, in contrast to the longer polymeric substrates such as RAX and sWAX [77].

Notably, hydrolysis occurred only with A^2XX and $A^{2,3}XX$, both of which carry arabinose substitutions at the O-2 position of xylose residues, whereas A^3X, substituted at O-3, was not hydrolyzed even after extended incubation. These results suggest that the PSA-3 xylanase aggregate preferentially attacks arabinose-substituted xylans from the non-reducing ends [71]. Such activity has been reported for specific xylanases with debranching capability ([69,71,72] . Taken together, these findings indicate that the debranching function of the PSA-3 xylanase aggregate may play an important role in the degradation of RAX and sWAX.

4. Materials and Methods#

4.1. Materials

Xylooligosaccharides, beechwood xylan (BWX), rye arabinoxylan (RAX), soluble wheat arabinoxylan (WAX), insoluble wheat arabinoxylan (iWAX) and carboxy methylcellulose 4M (CMC) were purchased from Megazyme, Denmark. A^2XX, $A^{2,3}XX$, and A^3X were also obtained from Megazyme. Xylose was purchased from Sigma Chemical, USA. HiTrap DEAE Sepharose FF column was obtained from Cytiva, Sweden. Xylans from sugarcane bagasse and Napier grass were prepared as described previously [78].

4.2. Enzyme Production by Solid-State Fermentation

Fusarium proliferatum PSA-3 was isolated from mango leaves as described previously [21]. Rice straw was used as growth substrate for solid-state fermentation. It was cut into small pieces and grounded in a blender to give particle sizes around 5 mm. Twenty-five grams of ground rice straw were placed in 5-L Erlenmeyer flasks and sterilized for 15 min at 121°C. To achieve a moisture content of 50%, the autoclaved rice straw was moistened with 50 mL sterilized tap water, and the moisture content was determined by a moisture analyzer. The rice straw medium was used for fungal cultivation.

Strain PSA-3 was routinely grown on potato-dextose agar (PDA). To initiate enzyme production by solid-state fermentation, 15 plugs, with 0.5-cm diameter, of active mycelia of strain PSA-3 grown on PDA (4-day culture) were taken and inoculated on rice straw at room temperature (25 ± 3 °C). After 7 days of fermentation, the enzyme was extracted by adding 200 mL of cold sodium-acetate buffer saline (ABS, 10 mM sodium-acetate and 137 mM NaCl, pH 5.5) to the growing culture. The culture suspension was shaken at 150 rpm for 1 h at room temperature and then filtered through a Whatman No. 1 using a vacuum pump to obtain liquid fraction. The solution was then centrifuged at 10,000 rpm at 4 °C for 20 min to remove fine particles, and it was considered crude protein extract.#

4.3. Determination of Protein

The protein concentration was determined by Bradford regent assay (BioRad, USA) following manufacturer's protocol with minor modification. Briefly, 200 µL of Bradford reagent was mixed with 20 uL of sample. The reaction mixture was then incubated for 10 min at room temperature, and the absorbance of the reaction was measured at 595 nm. Bovine serum albumin (BSA), with a concentration range of 0.05 mg/mL to 50 mg/mL, was used as standard.

4.4. Determination of Enzymatic Activities and Substrate Specificities

The xylanase and cellulase activities were determined based on the production of reducing sugars from RAX or CMC, respectively. The reaction mixture contained 8 µg of protein and 1% (w/v) substrate in ABS (pH 5.5), and the total volume of the reaction was adjusted to 200 µL. The reaction was incubated at 37 ºC for 15 min, stopped by placing the reaction tube in ice water bath, and centrifuged at 13,000 × g at 4 ºC for 10 min to separate the substrate from the liquid fraction.

 doi:10.20944/preprints202509.2067.v1

Reducing sugar in the liquid fraction was determined using the dinitrosalicylic acid (DNS) method [79] using glucose as the standard. In brief, 100 uL of liquid fraction was mixed 150 uL of DNS reagent, boiled for 10 min. and centrifuged at high speed. The liquid fraction was measured at an absorbance of 540 nm. One unit (U) of enzyme activity was defined as the amount of enzyme that releases 1 µmol of glucose reducing sugar equivalents per min under the assayed condition.

The substrate specificities of the enzyme towards different polysaccharides (1%, w/v): BWX, RAX, WAX, iWAX, and Avicel were tested. The enzymatic reaction was performed as described above, except for the Avicel that the incubation time was 24 h.

4.5. Xylanase Purification

4.5.1. Ammonium Sulfate Precipitation

To partially purify xylanase, one hundred milliliters of crude protein extract was treated with ammonium sulphate until 85% saturation reached. The mixture was kept at 4 ºC with mild stirring overnight to precipitate proteins. The protein was collected by centrifugation at 4 ºC, 8000 rpm for 15 min. The crude xylanase was then resuspended in 10 mL of ABS (pH 5.5) and dialyzed against the same buffer at 4 ºC with mild stirring overnight. The protein concentration before and after dialysis was determined by Bradford assay, and the enzyme activity was examined.

4.5.2. Ion-Exchange Chromatography

The purification was carried out with Fast protein liquid chromatography (FPLC) AKTA system, Amersham Biosciences (USA). To increase protein concentration, the enzyme solution was precipitated by cold (-20 ºC) acetone precipitation. The enzyme solution was mixed with cold acetone at a ratio of 1:4 and kept at -20 ºC for 1 h. After that, the mixture was centrifuged at 10,000 rpm for 15 min, and the precipitated protein was resuspended in 1 mL of ABS. Five hundred microliters of sample with a concentration of 3 mg/mL was then filtered through 0.22-µm syringe filter and loaded into a 1-mL HiTrap™ DEAE Sepharose FF column pre-equilibrated with 10 mM Tris-HCl buffer (pH 7.4). Enzyme elution was performed with sodium chloride (NaCl gradient (0 – 1 M) in the same buffer at a flow rate of 0.75 mL/min at room temperature. The sample was collected at 1 mL per fraction. Enzymatic activity and protein concentration in each fraction were determined.

4.5.3. Gel Filtration Chromatography

The protein purification was carried out with Fast protein liquid chromatography (FPLC) AKTA system, Amersham Biosciences (USA). Protein sample with a concentration of 0.75 mg/mLwas loaded into a Superdex TM 200 Increase 10/300 GL column. Enzyme elution was carried out at a flow rate of 0.75 mL/min by using 10 mM Tris-HCl buffer (pH 7.4). The sample was collected at 1 mL for each fraction. All fractions were determined for protein concentrations and assayed for enzymatic activity. Molecular weight standards include: Blue dextran (2,200 kDa, void volume), Thyroglobulin (669 kDa), Ferritin (440 kDa), Aldolasae (158 kDa), Conoalbumin (75 kDa), Ovalbumin (43 kDa), and Carbonic anhydrase (29 kDa)

4.6. Biochemical Characterization of Partially Purified Xylanase

4.6.1. Electrophoresis

10% Sodium dodecyl sulfate polyacrylamide gel electrophoresis (SDS-PAGE) under denaturing conditions was prepared according to []. Five micrograms of protein samples was mixed with 4x Laemmli sample buffer containing lithium dedocyl sulfate (LDS and 2-mercaptoethanol (Bio-Rad, USA) and boiled at 100 ºC for 10 min before being subjected to the gel for electrophoresis. The gel was strained with Coomassie Brilliant Blue R-250 to visualize the protein bands. The approximate

 doi:10.20944/preprints202509.2067.v1

molecular mass of the proteins was determined by calibration against broad range molecular weight markers using GangNam-STAIN™ Prestained Protein Ladder (iNtRON Biotechnology, South Korea)

In the case of protein stability analysis, samples were mixed with native sample buffer (no addition of LDS and β -mercaptoethanol) and treated at 90 ºC or 100˚C for 0, 1, 5, and 10 min. After that, the samples were subjected to 10% SDS-PAGE for electrophoresis, which was run at 200V for 45 min. The protein staining and molecular weight determination were performed as described above.

4.6.2. Zymogram

For in situ enzyme activity analysis, zymogram technique was used. Protein samples were prepared as described in the section 4.6.1 and loaded into 10% SDS-PAGE, which contained 0.2% (w/v) substrate (RAX or BWX). The gel was run at 100 V for 45 min. After electrophoresis, the gel was washed with 2% (v/v) Triton X-100 in 10 mM citrate buffer pH 6.0 for 20 min (repeated 2 times) and two times with buffer. After that, the gels were incubated with the same buffer at 37 ºC for 1 h and were stained with 1% (w/v) Congo red solution at room temperature for 15 min. The gels were destained with 1.0 M NaCl.

4.6.3. Effect of pH and Stability

The optimal pH of enzyme was determined at a various range of pHs from 3.0 to 9.0 at 37˚C for 15 min. The buffer systems used were sodium-citrate buffer (pH 3.0-7.0) and Tris-HCl buffer (pH 7.0-9.0). The reaction mixture contained 8 ug of protein and 1% (w/v) substrate (RAX or BWX) with a total volume of 200 uL. The reaction was performed at 37 ºC for 15 min, and the enzyme activity was determined. The pH stability was determined by adding an 8 µg of enzyme to different buffers, and the samples were then incubated at 4 ºC for 1 h. After that, the pH of the sample was adjusted to optimal pH (10 mM sodium-citrate buffer, pH 5.5) and the reaction was assayed at 37 ºC for 15 min to determine the residual activity.

4.6.4. Effect of Temperature and Stability

The optimal temperature of enzyme was determined in a range of temperature from 20 ºC to 60 ºC in an optimal buffer for 15 min. The reaction contained 8 ug of protein sample and 1% (w/v) substrate (RAX or BWX) with a total volume of 200 uL. After incubation, the enzyme activity was determined. Thermostability of enzyme was determined by incubating the enzyme (8 ug) in the optimal buffer at different temperatures (40 ˚C to 70 °C) for various times. The enzymes were taken at different time intervals and their residual enzyme activities were determined.

4.6.5. Effect of Metal Ion and Chemical Reagent

The effect of various metal ions, such as $CaCl_2$, $MgCl_2$, $CoCl_2$, $FeCl_2$, $NiCl_2$, LiCl, $CuSO_4$, $FeSO_4$, $ZnSO_4$, and EDTA at the final concentrations of 1 and 10 mM on enzymatic activity were determined using 1% (w/v) RAX and 1% (w/v) BWX as substrate. The 0.2 mL reaction mixture was incubated at 37˚C for 15 min. For the effect of other reagents included 2 and 5 mM β-mercaptoethanol, 1% and 5% (v/v) of Triton X-100, Tween 20, Tween 80, and SDS on the activity of enzyme, were studied. The reaction was preincubated with each reagent at 4ºC for 15 min. After that, the substrate was added and incubated at 37 ºC for 15 min. Finally, the effects of metal ions and chemical reagents with xylanase activity were determined by DNS assay.

4.6.6. Enzyme Kinetic (Michaelis-Menten Parameter)

RAX, sWAX and BWX were used as substrate, and 10 mM citrate buffer pH 6.0 was used as assay buffer. The reaction was incubated at 37 ºC, 300 rpm for 15 min. The released reducing sugar were assayed by DNS method. Michaelis-Menten constant (K_m) and maximum reaction velocity (V_{max}) were estimated using GraphPad Prism 9.0 software.

 doi:10.20944/preprints202509.2067.v1

4.7. Hydrolysis Products

The hydrolysis products from aggregated xylanase were measured by incubating an enzyme with substrate. Pure polysaccharides, including RAX, sWAX, iWAX, and BWX and extracted xylands from sugarcane bagasse Napier grass were used as the substrates for hydrolysis. The reactions were performed at 37 °C for 0, 5, 15, 30, 60, 120, and 160 min. The release of reducing sugar was determined by DNS assay. Thin layer chromatography (TLC) using silica gel 60 F_{254} plates was used to measure the hydrolysis products at various time intervals. As standards, xylose and xylooligosaccharides (X2–X6) were utilized. The products on TLC plates were developed using butanol: glacial acetic acid: distil water (2: 1: 1, v/v/v). The hydrolysis products were detected by spraying with Diphenylamine–Aniline–Phosphoric Acid reagent, followed by heating at 90 °C for 10 min.

For study xylanase mechanism, Xylobiose (X2), Xylotriose (X3), Xylotetraose (X4), Xylopentaose (X5) and Xylohexaose (X6) were used as chain oligomer substrates. A^2XX, $A^{2,3}XX$, and A^3X (Megazymes, Denmark) were used as branched oligomer substrates The reaction contained 0.2 mg/mL xylooligosaccharides, citrate buffer pH 6.0, and 8 µg enzyme, and incubated at 0, 1, 5, 15, and 30 min at 37 °C. The hydrolysis product was then performed on TLC plate and visualized.

5. Conclusions

This study provides new insight into the xylanolytic enzyme system of the pathogenic fungus *Fusarium proliferatum* PSA-3. A naturally occurring xylanase aggregate with strong activity against RAX and BWX was isolated from rice straw cultures and partially purified. SDS-PAGE and zymogram analyses under mild and denaturing conditions revealed at least four protein components within the aggregate, each displaying distinct modes of action on RAX and BWX. The aggregate showed remarkable resistance to several metal ions and thiol-containing compounds, and preferentially degraded highly substituted arabinoxylans such as RAX and sWAX over BWX. It retained activity across a broad pH range and elevated temperatures, underscoring its robustness. Hydrolysis product profiles from xylo-oligosaccharides (DP 2–6), purified xylans (RAX, sWAX, iWAX, and BWX), and extracted xylans from sugarcane bagasse and Napier grass demonstrated predominant endo-type activity, accompanied by debranching activity toward A^2XX and $A^{2,3}XX$. These findings expand our understanding of how multiple xylanases may assemble into functional aggregates, potentially enhancing enzyme stability and catalytic proximity. Such a mechanism may contribute to the ability of *Fusarium* to infect arabinoxylan-rich plant materials, including cereals and mango leaves. Altogether, this work highlights the role of xylanase aggregates in fungal pathogenesis and suggests that targeting these enzyme systems could inform strategies for antifungal development and sustainable disease management in agriculture.

Author Contributions: Conceptualization, P.P..; methodology, K.T. and P.P.; software, K.T..; validation, K.T., L.S. and P.P.; formal analysis, K.T. and P.P.; investigation, K.T. and P.P; resources, L.S. and S.A.; data curation, K.T.; writing—original draft preparation, K.T., L.S., S.A. and P.P.; writing—review and editing, K.C., T.W., and PP.; visualization, K.T. and P.P.; supervision, P.P..; funding acquisition, K.C., T.W. and P.P. All authors have read and agreed to the published version of the manuscript

Funding: This research was funded by the JASTIP-Net 2022 and 2023 program sponsored by Japan Science and TechnologyAgency (JST), JAPAN-ASEAN Science Technology Innovation Platform (JASTIP). Kanlaya Thatha gratefully thanks the support by the Petchra Pra Jom Kloa M.Sc. Research Scholarship, King Mongkut's University of Technology Thonburi, Thailand.

Data Availability Statement: The original contributions presented in this study are included in the article. Further inquiries can be directed to the corresponding authors.

Acknowledgments: Generative AI and AI-assisted technologies in the writing process. The authors declare the use of ChatGPT for English editing. After using this tool, the authors reviewed and edited the content as needed and took full responsibility for the content of the publication.

 doi:10.20944/preprints202509.2067.v1

Conflicts of Interest: The authors declare no conflict of interest.

References

1. Bhardwaj, N.; Kumar, B.; Verma, P. A detailed overview of xylanases: an emerging biomolecule for current and future prospective. *Bioresources and Bioprocessing* **2019**, *6*, doi:10.1186/s40643-019-0276-2.
2. Biely, P.; Singh, S.; Puchart, V. Towards enzymatic breakdown of complex plant xylan structures: State of the art. *Biotechnol Adv* **2016**, *34*, 1260–1274, doi:10.1016/j.biotechadv.2016.09.001.
3. Rennie, E.A.; Scheller, H.V. Xylan biosynthesis. *Curr Opin Biotechnol* **2014**, *26*, 100–107, doi:10.1016/j.copbio.2013.11.013.
4. Marcotuli, I.; Hsieh, Y.S.; Lahnstein, J.; Yap, K.; Burton, R.A.; Blanco, A.; Fincher, G.B.; Gadaleta, A. Structural Variation and Content of Arabinoxylans in Endosperm and Bran of Durum Wheat (Triticum turgidum L.). *J Agric Food Chem* **2016**, *64*, 2883–2892, doi:10.1021/acs.jafc.6b00103.
5. Ye, Z.H.; Zhong, R. Outstanding questions on xylan biosynthesis. *Plant Sci* **2022**, *325*, 111476, doi:10.1016/j.plantsci.2022.111476.
6. de O. Buanafina, M.M. Feruloylation in Grasses: Current and Future Perspectives. *Molecular Plant 2*, 861–872, doi:10.1093/mp/ssp067.
7. Zhang, B.; Zhong, Y.; Dong, D.; Zheng, Z.; Hu, J. Gut microbial utilization of xylan and its implication in gut homeostasis and metabolic response. *Carbohydr Polym* **2022**, *286*, 119271, doi:10.1016/j.carbpol.2022.119271.
8. Juturu, V.; Wu, J.C. Microbial xylanases: engineering, production and industrial applications. *Biotechnol Adv* **2012**, *30*, 1219–1227, doi:10.1016/j.biotechadv.2011.11.006.
9. Heinen, P.R.; Bauermeister, A.; Ribeiro, L.F.; Messias, J.M.; Almeida, P.Z.; Moraes, L.A.B.; Vargas-Rechia, C.G.; de Oliveira, A.H.C.; Ward, R.J.; Filho, E.X.F.; et al. GH11 xylanase from Aspergillus tamarii Kita: Purification by one-step chromatography and xylooligosaccharides hydrolysis monitored in real-time by mass spectrometry. *Int J Biol Macromol* **2018**, *108*, 291–299, doi:10.1016/j.ijbiomac.2017.11.150.
10. Chadha, B.S.; Kaur, B.; Basotra, N.; Tsang, A.; Pandey, A. Thermostable xylanases from thermophilic fungi and bacteria: Current perspective. *Bioresour Technol* **2019**, *277*, 195–203, doi:10.1016/j.biortech.2019.01.044.
11. Li, X.; Dilokpimol, A.; Kabel, M.A.; de Vries, R.P. Fungal xylanolytic enzymes: Diversity and applications. *Bioresour Technol* **2022**, *344*, 126290, doi:10.1016/j.biortech.2021.126290.
12. Gibson, D.M.; King, B.C.; Hayes, M.L.; Bergstrom, G.C. Plant pathogens as a source of diverse enzymes for lignocellulose digestion. *Curr Opin Microbiol* **2011**, *14*, 264–270, doi:10.1016/j.mib.2011.04.002.
13. Cruz-Davila, J.; Perez, J.V.; Castillo, D.S.D.; Diez, N. Fusarium graminearum as a producer of xylanases with low cellulases when grown on wheat bran. *Biotechnol Rep (Amst)* **2022**, *35*, e00738, doi:10.1016/j.btre.2022.e00738.
14. Moonjely, S.; Ebert, M.; Paton-Glassbrook, D.; Noel, Z.A.; Roze, L.; Shay, R.; Watkins, T.; Trail, F. Update on the state of research to manage Fusarium head blight. *Fungal Genet Biol* **2023**, *169*, 103829, doi:10.1016/j.fgb.2023.103829.
15. Tini, F.; Beccari, G.; Benfield, A.H.; Gardiner, D.M.; Covarelli, L. Role of the XylA gene, encoding a cell wall degrading enzyme, during common wheat, durum wheat and barley colonization by Fusarium graminearum. *Fungal Genet Biol* **2020**, *136*, 103318, doi:10.1016/j.fgb.2019.103318.
16. Bertonha, L.C.; Leal Neto, M.; Garcia, J.A.A.; Vieira, T.F.; Castoldi, R.; Bracht, A.; Peralta, R.M. Screening of Fusarium sp. for xylan and cellulose hydrolyzing enzymes and perspectives for the saccharification of delignified sugarcane bagasse. *Biocatalysis and Agricultural Biotechnology* **2018**, *16*, 385–389, doi:10.1016/j.bcab.2018.09.010.

 doi:10.20944/preprints202509.2067.v1

17. Dong, X.; Meinhardt, S.W.; Schwarz, P.B. Isolation and characterization of two endoxylanases from Fusarium graminearum. *J Agric Food Chem* **2012**, *60*, 2538–2545, doi:10.1021/jf203407p.
18. Heinen, P.R.; Caroline, H.; Rosane, M.P.; Adelar, B.R.d.C.G.S.; Jose, L.d.C.S.; Maria, d.L.T.M.P.; Marina, K.K. Xylanase from Fusarium heterosporum: Properties and influence of thiol compounds on xylanase activity. *African Journal of Biotechnology* **2014**, *13*, 1047–1055, doi:10.5897/ajb2013.13282.
19. Saha, B.C. Production, purification and properties of xylanase from a newly isolated *Fusarium proliferatum*. *Process Biochemistry* **2002**.
20. He, Y.; Zhou, X.; Li, J.; Li, H.; Li, Y.; Nie, Y. In Vitro Secretome Analysis Suggests Differential Pathogenic Mechanisms between Fusarium oxysporum f. sp. cubense Race 1 and Race 4. *Biomolecules* **2021**, *11*, doi:10.3390/biom11091353.
21. Bundidamorn, D.; Salaiphet, L.; Vichitsoonthonkul, T.; Ratanakhanokchai, K.; Phitsuwan, P. Screening of fungi isolated from damaged plant materials for the production of lignocellulolytic enzymes with decolorizing ability. *Asia-Pacific Journal of Science and Technology* **2021**, *26*, APST–26, doi:https://doi.org/10.14456/apst.2021.54.
22. Guo, Z.; Yu, Z.; Li, Q.; Tang, L.; Guo, T.; Huang, S.; Mo, J.; Hsiang, T.; Luo, S. Fusarium species associated with leaf spots of mango in China. *Microb. Pathog.* **2021**, *150*, 104736, doi:10.1016/j.micpath.2021.104736.
23. Paccanaro, M.C.; Sella, L.; Castiglioni, C.; Giacomello, F.; Martinez-Rocha, A.L.; D'Ovidio, R.; Schafer, W.; Favaron, F. Synergistic Effect of Different Plant Cell Wall-Degrading Enzymes Is Important for Virulence of Fusarium graminearum. *Mol Plant Microbe Interact* **2017**, *30*, 886–895, doi:10.1094/MPMI-07-17-0179-R.
24. Tundo, S.; Moscetti, I.; Faoro, F.; Lafond, M.; Giardina, T.; Favaron, F.; Sella, L.; D'Ovidio, R. Fusarium graminearum produces different xylanases causing host cell death that is prevented by the xylanase inhibitors XIP-I and TAXI-III in wheat. *Plant Sci* **2015**, *240*, 161–169, doi:10.1016/j.plantsci.2015.09.002.
25. Martinez-Pacheco, M.M.; Flores-Garcia, A.; Zamudio-Jaramillo, M.A.; Chavez-Parga, M.C.; Alvarez-Navarrete, M. Optimization of production of xylanases with low cellulases in Fusarium solani by means of a solid state fermentation using statistical experimental design. *Rev Argent Microbiol* **2020**, *52*, 328–338, doi:10.1016/j.ram.2019.12.003.
26. Huang, Y.; Busk, P.K.; Lange, L. Cellulose and hemicellulose-degrading enzymes in Fusarium commune transcriptome and functional characterization of three identified xylanases. *Enzyme Microb Technol* **2015**, *73-74*, 9–19, doi:10.1016/j.enzmictec.2015.03.001.
27. Faria, S.P.; de Melo, G.R.; Cintra, L.C.; Ramos, L.P.; Amorim Jesuino, R.S.; Ulhoa, C.J.; de Faria, F.P. Production of cellulases and xylanases by Humicola grisea var. thermoidea and application in sugarcane bagasse arabinoxylan hydrolysis. *Industrial Crops and Products* **2020**, *158*, doi:10.1016/j.indcrop.2020.112968.
28. Ezeilo, U.R.; Wahab, R.A.; Mahat, N.A. Optimization studies on cellulase and xylanase production by Rhizopus oryzae UC2 using raw oil palm frond leaves as substrate under solid state fermentation. *Renewable Energy* **2020**, *156*, 1301–1312, doi:10.1016/j.renene.2019.11.149.
29. Leschonski, K.P.; Kaasgaard, S.G.; Spodsberg, N.; Krogh, K.B.R.M.; Kabel, M.A. Two Subgroups within the GH43_36 α-l-Arabinofuranosidase Subfamily Hydrolyze Arabinosyl from Either Mono-or Disubstituted Xylosyl Units in Wheat Arabinoxylan. *International Journal of Molecular Sciences* **2022**, *23*, doi:10.3390/ijms232213790.
30. Li, T.; Wu, Q.; Wang, Y.; John, A.; Qu, H.; Gong, L.; Duan, X.; Zhu, H.; Yun, Z.; Jiang, Y. Application of Proteomics for the Investigation of the Effect of Initial pH on Pathogenic Mechanisms of Fusarium proliferatum on Banana Fruit. *Front Microbiol* **2017**, *8*, 2327, doi:10.3389/fmicb.2017.02327.

 doi:10.20944/preprints202509.2067.v1

31. Neves Junior, A.; Mansoldo, F.R.P.; Godoy, M.G.; Firpo, R.M.; Cedrola, S.M.L.; Vermelho, A.B. Production of an endo-polygalacturonase from Fusarium proliferatum isolated from agro-industrial waste. *Biocatalysis and Agricultural Biotechnology* **2021**, *38*, doi:10.1016/j.bcab.2021.102199.
32. Perincherry, L.; Urbaniak, M.; Pawlowicz, I.; Kotowska, K.; Waskiewicz, A.; Stepien, L. Dynamics of Fusarium Mycotoxins and Lytic Enzymes during Pea Plants' Infection. *Int J Mol Sci* **2021**, *22*, doi:10.3390/ijms22189888.
33. Perincherry, L.; Ajmi, C.; Oueslati, S.; Waskiewicz, A.; Stepien, L. Induction of Fusarium lytic Enzymes by Extracts from Resistant and Susceptible Cultivars of Pea (Pisum sativum L.). *Pathogens* **2020**, *9*, doi:10.3390/pathogens9110976.
34. Chang, K.F.; Hwang, S.F.; Conner, R.L.; Ahmed, H.U.; Zhou, Q.; Turnbull, G.D.; Strelkov, S.E.; McLaren, D.L.; Gossen, B.D. First report of Fusarium proliferatum causing root rot in soybean (Glycine max L.) in Canada. *Crop Protection* **2015**, *67*, 52–58, doi:10.1016/j.cropro.2014.09.020.
35. Faraz, A.; Haq, I.U.; Ijaz, S.; Mubeen, F.; Habib, A.; Qadri, R.W.K.; Khan, N.A. Morphgenomics based identification of Fusarium proliferatum causing Syagrus romanzoffiana wilt and exploitation of antifungal potential of Trichoderma species against this pathogen. *Journal of Plant Pathology* **2020**, *102*, 1097–1105, doi:10.1007/s42161-020-00572-9.
36. Lei, S.; Wang, L.; Liu, L.; Hou, Y.; Xu, Y.; Liang, M.; Gao, J.; Li, Q.; Huang, S. Infection and Colonization of Pathogenic Fungus Fusarium proliferatum in Rice Spikelet Rot Disease. *Rice Science* **2019**, *26*, 60–68, doi:10.1016/j.rsci.2018.08.005.
37. Das, S.P.; Ravindran, R.; Deka, D.; Jawed, M.; Das, D.; Goyal, A. Bioethanol production from leafy biomass of mango (Mangifera indica) involving naturally isolated and recombinant enzymes. *Prep. Biochem. Biotechnol.* **2013**, *43*, 717–734, doi:10.1080/10826068.2013.773342.
38. Sultan, A.; Frisvad, J.C.; Andersen, B.; Svensson, B.; Finnie, C. Investigation of the indigenous fungal community populating barley grains: Secretomes and xylanolytic potential. *J Proteomics* **2017**, *169*, 153–164, doi:10.1016/j.jprot.2017.03.009.
39. Saha, B.C. Purification and properties of an extracellular β-xylosidase from a newly isolated Fusarium proliferatum. *Bioresource Technology* **2002**, *90*, 33–38, doi:10.1016/s0960-8524(03)00098-1.
40. Shin, H.-D.; Chen, R.R. Production and characterization of a type B feruloyl esterase from Fusarium proliferatum NRRL 26517. *Enzyme and Microbial Technology* **2006**, *38*, 478–485, doi:10.1016/j.enzmictec.2005.07.003.
41. Chen, C.; Zhao, X.; Wang, X.; Wang, B.; Li, H.; Feng, J.; Wu, A. Mutagenesis of UDP-xylose epimerase and xylan arabinosyl-transferase decreases arabinose content and improves saccharification of rice straw. *Plant Biotechnol J* **2021**, *19*, 863–865, doi:10.1111/pbi.13552.
42. Yoshida, S.; Kusakabe, I.; Matsuo, N.; Shimizu, K.; Yasui, T.; Murakami, K. Structure of Rice-straw Arabinoglucuronoxylan and Specificity ofStreptomycesXylanase toward the Xylan. *Agric. Biol. Chem.* **2014**, *54*, 449–457, doi:10.1080/00021369.1990.10869948.
43. Mardetko, N.; Trontel, A.; Novak, M.; Pavlecic, M.; Ljubas, B.D.; Grubisic, M.; Tominac, V.P.; Ludwig, R.; Santek, B. Screening of Lignocellulolytic Enzyme Activities in Fungal Species and Sequential Solid-State and Submerged Cultivation for the Production of Enzyme Cocktails. *Polymers (Basel)* **2021**, *13*, doi:10.3390/polym13213736.
44. Prasoulas, G.; Gentikis, A.; Konti, A.; Kalantzi, S.; Kekos, D.; Mamma, D. Bioethanol Production from Food Waste Applying the Multienzyme System Produced On-Site by Fusarium oxysporum F3 and Mixed Microbial Cultures. *Fermentation* **2020**, *6*, doi:10.3390/fermentation6020039.

 doi:10.20944/preprints202509.2067.v1

45. Najjarzadeh, N.; Matsakas, L.; Rova, U.; Christakopoulos, P. Effect of Oligosaccharide Degree of Polymerization on the Induction of Xylan-Degrading Enzymes by Fusarium oxysporum f. sp. Lycopersici. *Molecules* **2020**, *25*, doi:10.3390/molecules25245849.
46. Amadi, O.C.; Egong, E.J.; Nwagu, T.N.; Okpala, G.; Onwosi, C.O.; Chukwu, G.C.; Okolo, B.N.; Agu, R.C.; Moneke, A.N. Process optimization for simultaneous production of cellulase, xylanase and ligninase by Saccharomyces cerevisiae SCPW 17 under solid state fermentation using Box-Behnken experimental design. *Heliyon* **2020**, *6*, e04566, doi:10.1016/j.heliyon.2020.e04566.
47. Ezeilo, U.R.; Lee, C.T.; Huyop, F.; Zakaria, II; Wahab, R.A. Raw oil palm frond leaves as cost-effective substrate for cellulase and xylanase productions by Trichoderma asperellum UC1 under solid-state fermentation. *J Environ Manage* **2019**, *243*, 206–217, doi:10.1016/j.jenvman.2019.04.113.
48. Marques, N.P.; de Cassia Pereira, J.; Gomes, E.; da Silva, R.; Araújo, A.R.; Ferreira, H.; Rodrigues, A.; Dussán, K.J.; Bocchini, D.A. Cellulases and xylanases production by endophytic fungi by solid state fermentation using lignocellulosic substrates and enzymatic saccharification of pretreated sugarcane bagasse. *Industrial Crops and Products* **2018**, *122*, 66–75, doi:10.1016/j.indcrop.2018.05.022.
49. de Amo, G.S.; Bezerra-Bussoli, C.; da Silva, R.R.; Kishi, L.T.; Ferreira, H.; Mariutti, R.B.; Arni, R.K.; Gomes, E.; Bonilla-Rodriguez, G.O. Heterologous expression, purification and biochemical characterization of a new xylanase from Myceliophthora heterothallica F.2.1.4. *Int J Biol Macromol* **2019**, *131*, 798–805, doi:10.1016/j.ijbiomac.2019.03.108.
50. Singh, G.; Samuchiwal, S.; Hariprasad, P.; Sharma, S. Melioration of Paddy Straw to produce cellulase-free xylanase and bioactives under Solid State Fermentation and deciphering its impact by Life Cycle Assessment. *Bioresour Technol* **2022**, *360*, 127493, doi:10.1016/j.biortech.2022.127493.
51. Yang, X.; Shi, P.; Huang, H.; Luo, H.; Wang, Y.; Zhang, W.; Yao, B. Two xylose-tolerant GH43 bifunctional beta-xylosidase/alpha-arabinosidases and one GH11 xylanase from Humicola insolens and their synergy in the degradation of xylan. *Food Chem* **2014**, *148*, 381–387, doi:10.1016/j.foodchem.2013.10.062.
52. Ohtsuki, T.; Suyanto; Yazaki, S.; Ui, S.; Mimura, A.; Suyanto. Production of large multienzyme complex by aerobic thermophilic fungus Chaetomium sp. nov. MS-017 grown on palm oil mill fibre. *Lett Appl Microbiol* **2005**, *40*, 111–116, doi:10.1111/j.1472-765X.2004.01644.x.
53. Phitsuwan, P.; Ratanakhanokchai, K. The recovery and bioproperties of a xylanolytic multi-enzyme complex from Tepidimicrobium xylanilyticum BT14. *Journal of Molecular Catalysis B: Enzymatic* **2015**, *120*, 28–37, doi:10.1016/j.molcatb.2015.06.007.
54. Phitsuwan, P.; Morag, E.; Tachaapaikoon, C.; Pason, P.; Kosugi, A.; Ratanakhanokchai, K. Behavior and supportive evidence of a large xylanase-containing multienzyme complex of tepidimicrobium xylanilyticum bt14. *BioResources* **2012**, *7*, 5934–5949.
55. van Dyk, J.S.; Sakka, M.; Sakka, K.; Pletschke, B.I. The cellulolytic and hemi-cellulolytic system of Bacillus licheniformis SVD1 and the evidence for production of a large multi-enzyme complex. *Enzyme and Microbial Technology* **2009**, *45*, 372–378, doi:10.1016/j.enzmictec.2009.06.016.
56. Jiang, Z.Q.; Deng, W.; Li, X.T.; Ai, Z.L.; Li, L.T.; Kusakabe, I. Characterization of a novel, ultra-large xylanolytic complex (xylanosome) from Streptomyces olivaceoviridis E-86. *Enzyme and Microbial Technology* **2005**, *36*, 923–929, doi:10.1016/j.enzmictec.2005.01.023.
57. Dou, T.Y.; Chen, J.; Liu, C. Isolation and subunit compositions of the xylanosome complexes produced by Cellulosimicrobium species. *Enzyme Microb Technol* **2020**, *133*, 109445, doi:10.1016/j.enzmictec.2019.109445.
58. Jiang, Z.; Dang, W.; Yan, Q.; Zhai, Q.; Li, L.; Kusakabe, I. Subunit composition of a large xylanolytic complex (xylanosome) from Streptomyces olivaceoviridis E-86. *J Biotechnol* **2006**, *126*, 304–312, doi:10.1016/j.jbiotec.2006.05.006.

 doi:10.20944/preprints202509.2067.v1

59. Duarte, M.; Alves, V.D.; Correia, M.; Caseiro, C.; Ferreira, L.M.A.; Romao, M.J.; Carvalho, A.L.; Najmudin, S.; Bayer, E.A.; Fontes, C.; et al. Structure-function studies can improve binding affinity of cohesin-dockerin interactions for multi-protein assemblies. *Int J Biol Macromol* **2022**, doi:10.1016/j.ijbiomac.2022.10.102.
60. Wang, W.; Yu, Y.; Dou, T.Y.; Wang, J.Y.; Sun, C. Species of family Promicromonosporaceae and family Cellulomonadeceae that produce cellulosome-like multiprotein complexes. *Biotechnol Lett* **2018**, *40*, 335–341, doi:10.1007/s10529-017-2469-0.
61. Dou, T.Y.; Luan, H.W.; Ge, G.B.; Dong, M.M.; Zou, H.F.; He, Y.Q.; Cui, P.; Wang, J.Y.; Hao, D.C.; Yang, S.L.; et al. Functional and structural properties of a novel cellulosome-like multienzyme complex: efficient glycoside hydrolysis of water-insoluble 7-xylosyl-10-deacetylpaclitaxel. *Sci Rep* **2015**, *5*, 13768, doi:10.1038/srep13768.
62. Hamann, P.R.V.; de, M.B.S.L.; Gomes, T.C.; Noronha, E.F. Assembling mini-xylanosomes with Clostridium thermocellum XynA, and their properties in lignocellulose deconstruction. *Enzyme Microb Technol* **2021**, *150*, 109887, doi:10.1016/j.enzmictec.2021.109887.
63. Sunna, A.; Antranikian, G. Xylanolytic enzymes from fungi and bacteria. *Crit. Rev. Biotechnol.* **1997**, *17*, 39–67.
64. Silva, L.A.O.; Terrasan, C.R.F.; Carmona, E.C. Purification and characterization of xylanases from Trichoderma inhamatum. *Electronic Journal of Biotechnology* **2015**, *18*, 307–313, doi:10.1016/j.ejbt.2015.06.001.
65. Sharma, S.; Verma, P.; Agrawal, K. Harnessing the potential of fungal xylanases: An insight into its application and technological advancements. *Industrial Crops and Products* **2024**, *222*, doi:10.1016/j.indcrop.2024.119967.
66. Polizeli, M.L.; Rizzatti, A.C.; Monti, R.; Terenzi, H.F.; Jorge, J.A.; Amorim, D.S. Xylanases from fungi: properties and industrial applications. *Appl Microbiol Biotechnol* **2005**, *67*, 577–591, doi:10.1007/s00253-005-1904-7.
67. Schmid, M.; Prinz, T.K.; Stabler, A.; Sangerlaub, S. Effect of Sodium Sulfite, Sodium Dodecyl Sulfate, and Urea on the Molecular Interactions and Properties of Whey Protein Isolate-Based Films. *Front Chem* **2017**, *4*, 49, doi:10.3389/fchem.2016.00049.
68. Garcia Medeiros, R.; Hanada, R.; Filho, E.X.F. Production of xylan-degrading enzymes from Amazon forest fungal species. *International Biodeterioration & Biodegradation* **2003**, *52*, 97–100, doi:10.1016/s0964-8305(02)00179-8.
69. Pauchet, Y.; Ruprecht, C.; Pfrengle, F. Analyzing the Substrate Specificity of a Class of Long-Horned-Beetle-Derived Xylanases by Using Synthetic Arabinoxylan Oligo- and Polysaccharides. *ChemBioChem* **2020**, *21*, 1517–1525, doi:10.1002/cbic.201900687.
70. Aronsson, A.; Guler, F.; Petoukhov, M.V.; Crennell, S.J.; Svergun, D.I.; Linares-Pasten, J.A.; Nordberg Karlsson, E. Structural insights of RmXyn10A - A prebiotic-producing GH10 xylanase with a non-conserved aglycone binding region. *Biochim Biophys Acta Proteins Proteom* **2018**, *1866*, 292–306, doi:10.1016/j.bbapap.2017.11.006.
71. Labourel, A.; Crouch, L.I.; Bras, J.L.; Jackson, A.; Rogowski, A.; Gray, J.; Yadav, M.P.; Henrissat, B.; Fontes, C.M.; Gilbert, H.J.; et al. The Mechanism by Which Arabinoxylanases Can Recognize Highly Decorated Xylans. *J Biol Chem* **2016**, *291*, 22149–22159, doi:10.1074/jbc.M116.743948.
72. Vardakou, M.; Flint, J.; Christakopoulos, P.; Lewis, R.J.; Gilbert, H.J.; Murray, J.W. A family 10 Thermoascus aurantiacus xylanase utilizes arabinose decorations of xylan as significant substrate specificity determinants. *J Mol Biol* **2005**, *352*, 1060–1067, doi:10.1016/j.jmb.2005.07.051.

 doi:10.20944/preprints202509.2067.v1

73. Liu, B.; Stevens-Green, R.; Johal, D.; Buchanan, R.; Geddes-McAlister, J. Fungal pathogens of cereal crops: Proteomic insights into fungal pathogenesis, host defense, and resistance. *J. Plant Physiol.* **2022**, *269*, 153593, doi:10.1016/j.jplph.2021.153593.
74. Sella, L.; Gazzetti, K.; Faoro, F.; Odorizzi, S.; D'Ovidio, R.; Schafer, W.; Favaron, F. A Fusarium graminearum xylanase expressed during wheat infection is a necrotizing factor but is not essential for virulence. *Plant Physiol Biochem* **2013**, *64*, 1–10, doi:10.1016/j.plaphy.2012.12.008.
75. Moscetti, I.; Tundo, S.; Janni, M.; Sella, L.; Gazzetti, K.; Tauzin, A.; Giardina, T.; Masci, S.; Favaron, F.; D'Ovidio, R. Constitutive expression of the xylanase inhibitor TAXI-III delays Fusarium head blight symptoms in durum wheat transgenic plants. *Mol Plant Microbe Interact* **2013**, *26*, 1464–1472, doi:10.1094/MPMI-04-13-0121-R.
76. Fülöp, L. The inhibition of xylanase enzymes by oligosaccharides produced during the degradation of biopolymers in biomass. *Biomass and Bioenergy* **2025**, *195*, doi:10.1016/j.biombioe.2025.107693.
77. Rudjito, R.C.; Jimenez-Quero, A.; Munoz, M.; Kuil, T.; Olsson, L.; Stringer, M.A.; Krogh, K.; Eklof, J.; Vilaplana, F. Arabinoxylan source and xylanase specificity influence the production of oligosaccharides with prebiotic potential. *Carbohydr Polym* **2023**, *320*, 121233, doi:10.1016/j.carbpol.2023.121233.
78. Khaire, K.C.; Sharma, K.; Thakur, A.; Moholkar, V.S.; Goyal, A. Extraction and characterization of xylan from sugarcane tops as a potential commercial substrate. *J Biosci Bioeng* **2021**, *131*, 647–654, doi:10.1016/j.jbiosc.2021.01.009.
79. MILLER, G.L. Use of Dinitrosalicylic Acid Reagent for Determination of Reducing Sugar. *Anal. Chem.* **1959**, *31*, 426–428,.